Presence of rapidly degrading permafrost plateaus in southcentral Alaska

Benjamin M. Jones[1], Carson A. Baughman[1], Vladimir E. Romanovsky[2,3], Andrew D. Parsekian[4], Esther L. Babcock[1], Eva Stephani[1], Miriam C. Jones[5], Guido Grosse[6], and Edward E. Berg[7]

[1] Alaska Science Center, U.S. Geological Survey, Anchorage, AK 99508, USA

[2] Geophysical Institute, University of Alaska Fairbanks, Fairbanks, AK 99775, USA

[3] Earth Cryosphere Institute, 86 Malygina Street, Tyumen 625000, Russia

[4] Department of Geology and Geophysics, University of Wyoming, Laramie, WY 82070, USA

[5] Eastern Geology and Paleoclimate Science Center, U.S. Geological Survey, Reston, VA 20192, USA

[6] Alfred Wegener Institute, Helmholtz Centre for Polar and Marine Research, Potsdam, 14473, Germany

[7] Kenai National Wildlife Refuge, U.S. Fish and Wildlife Service, Soldotna, AK 99669, USA (retired)

Correspondence to: Benjamin M. Jones (bjones@usgs.gov)

Abstract. Permafrost presence is determined by a complex interaction of climatic, topographic, and ecological conditions operating over long time scales. In particular, vegetation and organic layer characteristics may act to protect permafrost in regions with a mean annual air temperature (MAAT) above 0 °C. In this study, we document the presence of residual permafrost plateaus on the western Kenai Peninsula lowlands of southcentral Alaska, a region with a MAAT of 1.5±1 °C (1981–2010). Continuous ground temperature measurements between 16 September 2012 and 15 September 2015, using calibrated thermistor strings, documented the presence of warm permafrost (-0.04 °C to -0.08 °C). Field measurements (probing) on several plateau features during the fall of 2015 showed that the depth to the permafrost table averaged 1.48 m but at some locations was as shallow as 0.53 m. Late winter surveys (augering, coring, and GPR) in 2016 showed that the average seasonally frozen ground thickness was 0.45 m, overlying a talik above the permafrost table. Measured permafrost thickness ranged from 0.33 m to >6.90 m. Manual interpretation of historic aerial photography acquired in 1950 indicates that residual

permafrost plateaus covered 920 ha as mapped across portions of four wetland complexes encompassing 4,810 ha. However, between 1950 and ca. 2010, permafrost plateau extent decreased by 60.0 %, with lateral feature degradation accounting for 85.0 % of the reduction in area. Permafrost loss on the Kenai Peninsula is likely associated with a warming climate, wildfires that remove the protective forest and organic layer cover, groundwater flow at depth, and lateral heat transfer from wetland surface waters in the summer. Better understanding the resilience and vulnerability of ecosystem-protected permafrost is critical for mapping and predicting future permafrost extent and degradation across all permafrost regions that are currently warming. Further work should focus on reconstructing permafrost history in southcentral Alaska as well as additional contemporary observations of these ecosystem-protected permafrost sites lying south of the regions with relatively stable permafrost.

1 Introduction

Permafrost is a major component of the cryosphere in the northern hemisphere, covering ~24 % of the terrestrial landscape (Brown et al., 1998). Permafrost is defined as ground that remains at or below 0 °C for at least two consecutive years (Van Everdingen, 1998). Four zones describe the lateral extent of permafrost regions: continuous (90–100 %), discontinuous (50–90 %), sporadic discontinuous (10–50 %), and isolated discontinuous (<10 %). This zonation typically represents the north to south changes in spatial distribution for terrestrial permafrost in high latitudes. Mean annual ground temperatures (MAGT) in the continuous permafrost zone can be as cold at -15 °C, fall within a narrow range around -2 °C in the discontinuous permafrost zone, and can be warmer than -1 °C in sporadic and isolated permafrost zones (Smith and Riseborough, 2002; Romanovsky et al., 2010; Smith et al., 2010). In the absence of extensive ground temperature data, researchers have estimated the southern limit of permafrost in northern high latitudes with continental-scale patterns of air temperature isotherms (Brown, 1960, 1970; Ferrians, 1965; Brown et al., 1998). However, in reality complex interactions between climatic,

55 topographic, hydrologic, and ecologic conditions operating over long time scales regulate

56 permafrost presence and stability (Shur and Jorgenson, 2007). Due to these interactions,

57 permafrost may persist in regions with a mean annual air temperature (MAAT) above 0 °C, and

58 it may degrade in regions with a MAAT below -10 °C (Jorgenson et al., 2010). Thus, the extent

59 and dynamics of permafrost and permafrost-related landscape features remain poorly mapped

60 and modelled at sufficiently fine resolution needed for predicting the impact of climate change

61 on specific local landscapes, which is necessary for many decision makers.

62   Permafrost warming, degradation, and thaw subsidence can have significant implications

63 for ecosystems, infrastructure, and climate at local, regional, and global scales (Jorgenson et al.,

64 2001; Nelson et al., 2001; Schuur et al., 2008). In general, permafrost in Alaska has warmed

65 between 0.3–6.0 °C since ground temperature measurements began between the 1950–1980s

66 (Lachenbruch and Marshall, 1986; Romanovsky and Osterkamp, 1995; Romanovsky et al., 2002;

67 Osterkamp, 2007; Romanovsky et al., 2010). Warming and thawing of near-surface permafrost

68 may lead to widespread terrain instability in ice-rich permafrost in the Arctic (Jorgenson et al.,

69 2006; Lantz and Kokelj, 2008; Gooseff et al., 2009; Jones et al., 2015; Liljedahl et al., 2016) and

70 the sub-Arctic (Osterkamp et al., 2000; Jorgenson and Osterkamp, 2005; Lara et al., 2016). Such

71 land surface changes can impact vegetation, hydrology, aquatic ecosystems, and soil-carbon

72 dynamics (Grosse et al., 2011; Jorgenson et al., 2013; Kokelj et al., 2015; O'Donnell et al., 2011;

73 Schuur et al., 2008; Vonk et al., 2015). For example, in boreal peatlands, thaw of ice-rich

74 permafrost often converts forested permafrost plateaus into lake and wetland bog and fen

75 complexes (Camill, 1999; Jorgenson et al., 2001; Payette et al., 2004; Sannel and Kuhry 2008;

76 Sannel and Kuhry, 2011; Quinton et al., 2011; Jorgenson et al., 2012; Kanevskiy et al., 2014;

77 Swindles et al., 2015; Lara et al., 2016). Furthermore, the transition from permafrost peatlands

78   to thawed or only seasonally frozen peatlands can have a positive or a negative feedback on

79   regional and global carbon cycles depending on permafrost conditions and differential effects of

80   thaw on net primary productivity and heterotrophic respiration (Turetsky et al., 2007; Swindles

81   et al., 2015), as well as on the degree of loss of the former deep permafrost carbon pool

82   (O'Donnell et al., 2012).

83   In Alaska, a variety of permafrost conditions shape roughly 80 % of the landscape

84   (Jorgenson et al., 2008). Shur and Jorgenson (2007) proposed five classes of permafrost that

85   describe the interaction of climatological and ecological processes. Arranged from coldest to

86   warmest, these permafrost classes are as follows: climate-driven; climate-driven but ecosystem-

87   modified; climate-driven but ecosystem-protected; ecosystem-driven; and ecosystem-protected.

88   Ecosystem-protected permafrost is the warmest and most vulnerable of the five classes of

89   permafrost and characterizes the sporadic and isolated permafrost zones. It comprises residual

90   permafrost that persists due to favourable ecosystem factors under a climate that is not conducive

91   to its formation. Press disturbances, associated with warming air temperatures and increases in

92   precipitation (especially snow), and pulse disturbances, such as fire or human activities, can

93   trigger immediate ecosystem modification and permafrost thaw in these regions (Shur and

94   Jorgenson, 2007).

95   Since permafrost acts as a sentinel, integrator, and regulator of climate change, improved

96   understanding of its distribution and dynamics is essential, particularly along the southern

97   permafrost boundary (Lunardini, 1996). Southcentral Alaska, a region with a MAAT ~2 °C, is

98   typically mapped as being within the permafrost-free zone (Ferrians, 1965; Brown et al., 1998;

99   Pastick et al., 2015). However, ecosystem-protected permafrost persists in southcentral Alaska

100   in regions with present-day climatic conditions that are no longer conducive to its formation

4

101   (Shur and Jorgenson, 2007). Isolated permafrost patches in southcentral Alaska exist on the

102   western Kenai Peninsula Lowlands (Berg et al., 2009; Hopkins et al., 1955; Jorgenson et al.,

103   2008) and in the vicinity of Anchorage (Jorgenson et al., 2003; Riddle and Rooney, 2012;

104   Kanevskiy et al., 2013). Enhanced insight into the resilience and vulnerability of ecosystem-

105   protected permafrost is important due to its utility as a climate indicator and a forecaster of the

106   environmental consequences expected to arise from permafrost thaw elsewhere in the boreal

107   forest where MAAT is expected to warm beyond 0 °C in the coming decades (Beilman et al.,

108   2001). Nevertheless, to date, detailed studies of these southcentral Alaska ecosystem-protected

109   permafrost deposits have remained limited (Kanevskiy et al., 2013).

110   This study documents the presence of rapidly degrading permafrost plateaus on the

111   western Kenai Peninsula lowlands of southcentral Alaska (Fig. 1), a region with a MAAT of

112   1.5 ± 1 °C (Fig. 2). In mid-September 2012, we conducted field studies at several black spruce

113   plateaus located within herbaceous wetland complexes. Continuous ground temperature

114   measurements between 16 September 2012 and 15 September 2015 confirmed the presence and

115   degradation of permafrost. Probing, drilling, coring, and ground-penetrating radar surveys

116   conducted in the summer, fall, and winter seasons provided additional information on the

117   geometry of the frozen ground below the forested plateaus. Historic aerial photography and high-

118   resolution satellite imagery from 1950, 1984, 1996, and ca. 2010 were also used to map decadal-

119   scale changes in the aerial extent of the residual permafrost plateaus in portions of four wetland

120   complexes on the western Kenai Peninsula. This study aims to document and incorporate the

121   loss of ecosystem-protected permafrost into the overall understanding of landscape dynamics on

122   the western Kenai Peninsula lowlands. More importantly, insights into its stability will enhance

123 mapping and predicting current and future permafrost extent along the southern fringe of the

124 circumpolar permafrost region.

2 Study Area

126 The western Kenai Peninsula lowlands are located in southcentral Alaska, between 59.6–61.0

127 °N, and are generally less than 100 m above sea level (asl) (Fig. 1). The lowlands experience a

128 semi-continental climate due to a rain shadow produced by the Kenai Mountains to the east and

129 the presence of Cook Inlet to the west and north, and Kachemak Bay to the south (Jones et al.,

130 2009). Regional MAAT for 1981–2010 was 1.5 °C, with a mean annual precipitation of 441 mm

131 (http://www.ncdc.noaa.gov/crn/observations.htm) (Fig. 2). The lowlands represent a unique

132 landscape where two major glacial ice fields converged during the Late Wisconsin, 25,000–

133 21,000 kya (Reger et al., 2007). The modern topography, composed of moraines, outwash fans,

134 kettle lakes, kames, and eskers, is indicative of this glacial history (Hopkins et al., 1955). During

135 the Holocene, the Kenai Peninsula lowlands have succeeded to boreal forest, muskeg, and

136 wetlands laced with rivers and creeks and dotted with lakes (Anderson et al., 2006; Reger et al.,

137 2007). Pastick et al. (2015) recently mapped this region as being permafrost-free in the upper

138 one meter of the ground surface.

139 The Kenai lowlands are situated in an ecotone between the coastal temperate rainforest

140 and interior boreal forest. Species assemblages depend on topography and disturbance history,

141 as well as their location relative to the rain shadow. Black spruce (*Picea mariana*), white spruce

142 (*Picea glauca*), Sitka spruce (*Picea sitchensis*), Lutz spruce (*Picea x lutzii,* hybrid of white and

143 Sitka spruce), paper birch (*Betula kenaica*), alder (*Alnus sp.*), black cottonwood (*Populus*

144 *trichocarpa*), and aspen (*Populus tremuloides*) all occur within various forest stand types.

145 Herbaceous and woody wetland complexes intermingle with these forests in low-lying areas and

146 river corridors. Within wetland complexes, elevated forested plateaus, primarily black spruce

147 but with some paper birch and cottonwood and an understory of dwarf shrubs, exist where the

148 ground surface has been elevated above the regional water table. We suspected these features

149 were associated with a volumetric expansion of freezing peat, forming a permafrost plateau, an

150 elevated permafrost feature associated with frost heave (Zoltai, 1972, Zoltai, 1993).

151 Characterization of degrading permafrost plateaus is the focus of our studies on the Kenai

152 Peninsula.

153 **3 Methods**

154 In September 2012, we conducted field studies at a number of black spruce plateaus located

155 within herbaceous wetland complexes (Fig. 1, Fig. 3). These studies documented frozen ground

156 below an unfrozen layer with thicknesses ranging from 0.49m to >1.00 m. The plateau features

157 tended to have sharply defined scalloped edges, marginal thermokarst moats, and collapse-scar

158 depressions on their summits (Fig. 3). These traits were characteristic of the permafrost features

159 described by Hopkins et al. (1955) on the Kenai Peninsula and similar to permafrost plateaus

160 across colder boreal regions (Zoltai, 1972; Thie, 1974; Jorgenson et al., 2001; Camill, 2005;

161 Sannel et al., 2015). To answer whether the frozen deposits encountered at the black spruce

162 plateaus were indeed permafrost, we collected continuous ground temperature measurements for

163 three years, measured late-summer thaw depths, mechanically drilled and cored for the base of

164 the frozen ground, imaged the subsurface with ground-penetrating radar (GPR), and analysed a

165 time series of high-resolution remotely sensed imagery. These research efforts are described in

166 more detail below.

3.1 Field Instrumentation and Surveys

To confirm the presence or absence of permafrost, data loggers were installed on 12 September 2012 at one ground temperature monitoring site in the Browns Lake and at three sites in the Watson Lake area (Fig. 1). A 5 cm diameter Kovacs Enterprise ice auger was used to drill the boreholes and cased the holes with a 4.5 cm outer-diameter polyvinyl chloride (PVC) tube from the base of the borehole to within 10 cm of the surface. Each site was instrumented with a four channel Hobo data logger (Onset U12-008) buried below the ground surface (bgs). The data loggers recorded hourly ground temperature at four depths from 0.10–3.00 m bgs using Hobo TMC1-HD and TMC2-HD thermistors (Table 1). The manufacturer-specified accuracy of the thermistors is ±0.25 °C. Prior to deployment, we placed the data logger thermistors in a 0°C ice bath for up to 45 minutes to estimate a calibration factor for post-processing of the data following download in the field. After calibration in a 0°C ice bath, the precision of temperature measurements near 0 °C is limited only by the sensor-logger system sensitivity, which is 0.031 °C in this case. Therefore, the temperatures in our case were measured with the precision better than +/- 0.02 °C and changes in soil temperature exceeding 0.031 °C can be recorded properly using this measuring system. This fact was established and demonstrated many times during our measurements in deeper boreholes using similar measuring systems when the annually measured temperature in some boreholes at deeper depths (50 m and deeper) will remain constant. These calibration techniques and measurement sensitivities are similar to improvements recorded for other measurement systems (Sannel et al., 2015; Cable et al., 2016). All data were post-processed prior to summarizing the hourly ground temperature data into daily, monthly, and annual means.

189   Additional field surveys at each study site provided information on the geometry of the

190   frozen ground distribution and deposit types. A tile probe was used to measure the depth to

191   frozen sediments at each ground temperature monitoring location in mid-September 2015

192   (limited to 2.2 m bgs). At the two forested plateaus in the Watson Lake wetland complex, tile

193   probing locations were selected randomly and split between hummock and depression

194   microtopography. At the Browns Lake site, this depth was recorded at three points every meter

195   along a 100 m transect across the plateau feature. In addition, a topographic profile of the

196   primary Browns Lake plateau was collected using a Leica survey-grade differential GPS (dGPS)

197   system ($\pm$0.02 m vertical accuracy) on 09 October 2015 to adjust the probing measurements

198   relative to the local topography. An additional dGPS profile was acquired on 19 February 2016

199   at an adjacent plateau to provide more relative feature height information in the wetland

200   complex. At both the Browns Lake and Watson Lake locations, the frozen ground thickness was

201   measured using the Kovacs Enterprise ice auger system powered by an 18V portable drill. At

202   Browns Lake (site PF-BL-6), a borehole was also core-drilled to a depth of 5.38 m using a

203   SIPRE permafrost corer (5 cm diameter) with an engine auger head for analysis of the frozen

204   ground deposit (Fig. 1). The frozen cores were described according to the cryofacies method

205   (French and Shur, 2010) using cryostructure classification systems inspired from Murton and

206   French (1994) and Kanevskiy et al. (2014). Gravimetric ice contents of eleven samples were

207   measured by oven drying at 60 °C for 168 hours. Volumetric ice contents were measured from

208   ten well-preserved samples.

209   Implementation of GPR allowed to image certain characteristics of the frozen ground

210   along the primary Browns Lake plateau feature. A shielded 100 MHz Mala antenna was used in

211   July 2014 and Sensors & Software 100 MHz unshielded bi-static antennas in common-offset

212 configuration in February 2016. The data were processed using commercially available Reflex-

213 W processing software (Sandmeier, 2008). Basic processing steps included dewow, time-zero

214 correction, removing bad traces, and bandpass filtering (40–67.2–128–369 MHz for Mala; 25–

215 50–200–400 MHz for Sensors & Software). Additional processing steps included an average

216 background subtraction with a running window of 20–100 traces to reduce noise from surface

217 multiples, where applicable, and variable gain for viewing purposes. Care was taken during

218 processing to preserve any flat-lying reflectors. Finally, the radargrams were corrected using the

219 dGPS surface topography and converted two-way travel time to depth using an estimated

220 average subsurface velocity of 0.038 m ns^{-1} calibrated to average direct probe depths.

3.2 Remotely Sensed Imagery and Change Detection

222 Historic aerial photography and contemporary high resolution satellite imagery acquired between

223 1950–ca. 2010 provided an estimated extent of forested plateaus centred on four wetland

224 complexes on the western Kenai Peninsula lowlands. Four change detection study areas (Fig. 1)

225 were selected based on the presence of forested-plateau features surrounded by herbaceous

226 wetland vegetation that likely indicated permafrost presence in the boreal wetlands on the Kenai

227 Peninsula (Hopkins et al., 1955). Arranged from north to south, these included portions of the

228 Mystery Creek, Watson Lake, Browns Lake, and Tustumena Lake wetland complexes (Fig. 1).

229 Mapping forested plateau features and their change over time is a common method for detection

230 of permafrost thaw in boreal wetlands. The land cover change associated with conversion of a

231 forested permafrost plateau to a lake or herbaceous wetland (i.e. bog or fen) is readily detectable

232 in high-resolution remotely sensed imagery (Thie, 1974; Camill and Clark, 1998; Osterkamp et

233 al., 2000; Jorgenson et al., 2001; Jorgenson et al., 2008; Payette et al., 2004; Quinton et al., 2011;

234 Lara et al., 2016).

235   A 25 km^2 square study area was overlaid at each of the potential permafrost areas and

236   clipped the wetland extent as defined by the 2001 National Land Cover Dataset for Alaska

237   (http://www.mrlc.gov/nlcd2011.php) to define the mapping area.   Panchromatic, Digital

238   Orthophoto Quadrangle (DOQs) images were produced at a spatial resolution of 1.0 m for the

239   entire Kenai Peninsula between July–August 1996. The DOQs provided the base upon which to

240   georegister the other remotely sensed image datasets that consisted of panchromatic aerial photos

241   collected in August 1950 (1:40,000 scale), color-infrared aerial photos acquired in 1984

242   (1:62,500 scale), and panchromatic high-resolution satellite images (<1 m spatial resolution)

243   acquired in ca. 2010. The mean RMS error associated with image georegistration was 1.82 m

244   and ranged from 1.32–2.61 m.   All images were sampled to a ground resolution of 1 m.

245   Following image registration, forested plateaus were manually digitized in a Geographic

246   Information System (ArcGIS v. 10.1) at a mapping scale of 1:1,000 (Fig. 4). The high-spatial

247   resolution, georegistered remotely sensed datasets allowed for the assessment of residual

248   permafrost plateau extent in four time slices (1950, 1984, 1996, ca. 2010) and change rates

249   across three decadal-scale time periods: (1) 1950–1984 (34 years), (2) 1984–1996 (12 years), and

250   (3) 1996–ca. 2010 (14 years).

251   **3.3 Climate and Weather Data**

252   Climate and weather data were compiled from two regional stations to provide context for

253   interpreting the ground thermal regime data and changes mapped in the remotely sensed data.

254   Hourly air temperature data were compiled from Kenai Municipal Airport (KMA) (WBAN:

255   26523) for 1948–1971 and 1973–Present and sub-hourly air temperature data from the Kenai 29

256   ENE station (WBAN:26563) located at the Alaska Department of Fish and Game Moose

257   Research Center (MRC) from September 2010–Present.   Since the MRC station is more

258 representative of the field study sites, the temperature record for MRC were reconstructed back

259 to 1948 using a linear regression function found between KMA and MRC daily mean

260 temperatures as summarized from hourly and sub-hourly measurements. The regression

261 equation was calculated by comparing daily mean temperature for 1 January 2012 to 31

262 December 2015, and validated against daily mean temperatures at the MRC for 1 September

263 2010 to 31 December 2011. Lastly, daily snow depth totals were acquired from September

264 2012–September 2015 from MRC records (http://wcc.sc.egov.usda.gov/nwcc/site?sitenum=966).

265 **4 Results**

266 **4.1 Ground thermal regime of southcentral Alaska permafrost**

267 Calibrated ground temperature records collected between 16 September 2012 and 15 September

268 2015 at one forested plateau near Browns Lake and two forested plateaus near Watson Lake

269 confirmed the presence of near-surface permafrost on the western Kenai Peninsula lowlands

270 (Fig. 5a–5c). Over this time period, the MAGT of permafrost at 1.0 m bgs ranged from -0.04 °C

271 to -0.08°C (Table 1). At the Browns Lake PF1 and the Watson Lake PF2 sites, permafrost at 2.0

272 m bgs had a MAGT between -0.06 °C and -0.08 °C. At the Browns Lake PF1 site, permafrost at

273 3.0 m bgs had a MAGT between -0.07 °C and -0.08 °C (Table 1). No permafrost was detected at

274 a black spruce forested, non-plateau site near Watson Lake between September 2012 and August

275 2014 (Fig. 5d).

276 During the three-year observation period, an increase in near-surface ground

277 temperatures was recorded at all three permafrost sites in response to increases in air temperature

278 (Table 1, Fig. 5). The ground temperature at 0.5 m depth was substantially below 0 °C at all

279 three sites during the 2012–2013 winter with minimum temperatures between -1.33 °C (Browns

280   Lake) and -2.50 °C (Watson Lake PF2). In the 2013–2014 winter, the ground at 0.5 m depth was

281   barely frozen at the Browns Lake and Watson Lake PF1 sites (Fig. 5a and 5b), with minimum

282   winter temperatures at -0.32 °C and -0.20 °C, respectively. The increase in summer ground

283   temperatures at 0.5 m depth was also substantial. By the end of the 2012 warm period, this

284   temperature was above 0 °C only at the Browns Lake site (the maximum was at 0.40 °C). At the

285   Watson Lake PF1 and PF2 sites the temperature at 0.5 m depth was just below 0 °C and never

286   exceeded the thawing threshold, indicating that the maximum summer thaw (the active layer

287   thickness) was just below 0.5 m during 2012. However, during the summer of 2013 and 2014,

288   the active layer thickness was more than 0.5 m at both of these sites and the maximum

289   temperatures in 2014 exceeded 1 °C at the Watson Lake sites (Fig. 5b and 5c). At the Browns

290   Lake site the temperature at 0.5 m depth reached almost 2 °C before the thermistor malfunction.

291   The ground temperature warming at 0.5 m depth continued in 2015 (Fig. 5b and 5c).

292   The increase in the shallow ground temperatures triggered warming in the near-surface

293   permafrost at all three permafrost sites (Fig. 6). This warming was strong enough to initiate top-

294   down permafrost thaw at the Watson Lake PF1 site in the fall of 2014 (Fig. 6b). Sensor failure

295   during the winter of 2014–2015 prevented further observations of ground temperature at this site

296   following thaw that winter. At the Watson Lake PF2 site bottom-up permafrost thaw was

297   detected at a depth of 2 m during the fall of 2015 and likely associated with groundwater flow or

298   degradation of the permafrost in the thermokarst moat that borders the plateau. At the Browns

299   Lake site permafrost persisted at the depths between 1.0–3.0 m bgs over the three-year

300   observation period (Fig. 6a). However, MAGT warmed by 0.02 °C to 0.01 °C at all three depths

301   during the observation period. The temperature at 1.0 m bgs is only -0.04 °C now.

4.2 Depth to permafrost table and permafrost thickness

The thaw depth at the data logger observation sites, as measured with the tile probe on 16 September 2015, was 0.64 m for the Watson Lake PF1 site (n=3), 0.53 m for the Watson Lake PF2 site (n=6), and 0.57 m for the Browns Lake PF1 site (n=6). More systematic probing at all three sites on 16 September 2015 showed that the average depth to the permafrost table where detectable (max probe length=2.20 m) was 1.48 m (n=222). However, probing did not encounter frozen ground in the upper 2.20 m of the ground surface at an additional 140 measurement points, mostly associated with collapse-scar features and thermokarst moats. In general, depth to the permafrost table depended on the local topographic conditions at each site. Hummocks (n=164) tended to have a shallower depth to the permafrost table where measureable (average of 1.12 m), while depth to the permafrost table measurements in depressions (n=58) was larger (average of 1.53 m).

The measurements of the depth to permafrost table were complemented with mechanical augering, coring, and GPR surveys in July 2014, September 2015, and February 2016 to constrain permafrost thickness at the field observation sites. The most detailed measurements were collected at the Browns Lake PF1 plateau feature (Fig. 7a). At this site, a topographic survey of the plateau feature was conducted to plot depth to permafrost table along with seasonally frozen depth and constraints on permafrost thickness in relation to the relative ground surface elevation along a 100 m transect (Fig. 7b). The relative mean elevation of the plateau above the surrounding wetland area and the collapse-scar bog in the center was 0.49 m, with a maximum along the transect of 0.95 m, and a maximum across the feature of 1.30 m. A topographic survey on an adjacent plateau feature produced a mean relative height of 0.59 m and a maximum of 1.81 m. We measured permafrost thickness at five locations and minimum-limiting permafrost thicknesses at another five locations along the Browns Lake primary plateau

feature, with one limiting thickness measurement at an adjacent plateau feature using the Kovacs auger. The base of the permafrost at the two marginal plateau measurement sites at the primary plateau feature indicated a permafrost thickness of 0.45 m and 0.33 m (Fig. 7b). At the three interior plateau measurements points, permafrost was 5.57–5.65 m thick. At one of these locations (0.98 m relative height), a core was acquired. It consisted of frozen peat from 0.48–5.69 m bgs, overlying 0.25 m of unfrozen peat, with unfrozen mineral sediment at the base. At the other five locations where the bottom of permafrost was not reached, drilling operations documented permafrost at least down to between 3.5–4.0 m bgs (Fig. 7b), and contained frozen peat as well.

The permafrost core at the PF-BL-6 site was described as poorly decomposed peat with well-developed organic-matrix cryostructures, except between depths of 3.32–3.65 m where a layer of silt and peat with mainly microlenticular cryostructure was observed (Fig. 8 and 9). The gravimetric and volumetric ice contents of the peat varied between 883–1873 % and 80–96 %, respectively, while they were 379–447 % and 81 %, respectively, in the previously mentioned silt and peat layer. The upper two meters of peat were characterized mainly by an organic-matrix porphyritic cryostructure transitioning to an organic-matrix microlenticular cryostructure with some layered ice lenses. Below two meters, the peat was characterized mainly by an organic-matrix microlenticular cryostructure with some belt-like and suspended cryostructures.

GPR surveys conducted in July 2014 and February 2016 provided more continuous information on the geometry associated with the permafrost table in the residual plateaus on the primary Browns Lake plateau feature (Fig. 10). The topography-corrected radargrams show a prominent reflector between 1–3 m depth that coincides with the permafrost table in both the summer (Fig. 10a) and winter (Fig. 10b) survey. The center portion of both images is

349 characterized by moderately continuous and chaotic reflectors (Neal, 2004), as expected for

350 records in unfrozen peat sequences (Parsekian et al., 2010) associated with the collapse-scar bog.

351 The areas underlain by permafrost (i.e. 0–30 m, 60–90 m) show subdued reflection events deeper

352 than the permafrost table; however, we were unable to image the permafrost base. The

353 interpretation of these radargrams provides lateral subsurface information on the presence of a

354 talik overlying the permafrost table.

355 **4.3 Remote identification of permafrost plateaus**

356 In 1950, residual permafrost plateau extent accounted for 920 ha of the 4,810 ha (19.1 %) of

357 wetlands mapped within four change detection areas (Fig. 1, Table 2). Between 1950 and 1984,

358 permafrost plateau extent decreased to 750 ha, at an average rate of 5.1 ha yr^{-1} (Table 3).

359 Between 1984–1996, permafrost extent dropped to 520 ha, at an average rate of 18.8 ha yr^{-1}, the

360 greatest rate documented in the study periods. Between 1996–2010, permafrost features

361 continued to degrade at a rate of 9.5 ha yr^{-1} so that by 2010, only 370 ha of the permafrost

362 features remained. Thus, between 1950–ca. 2010, 60 % of the residual permafrost plateaus

363 disappeared in the mapped study areas (Fig. 11 and Table 2).

364 Assessment of change in the four wetland complexes showed differences in the extent

365 and change rate of residual permafrost plateaus overtime. The Mystery Creek study area had the

366 most extensive permafrost plateau coverage (32.8 % of the wetland area analysed) in the 1950s

367 relative to the Watson Lake (9.8 %), Browns Lake (11.1 %), and Tustumena Lake (15.8 %) study

368 areas (Table 2). By ca. 2010, permafrost plateau extent in each of the study areas diminished to

369 a cover of 14.8 %, 3.5 %, 3.8 %, and 5.2 %, respectively. Thus, there was a loss of 54.8 % of the

370 plateau extent in the Mystery Creek study area, 64.7 % in the Watson Lake study area, 65.5 % in

371 the Browns Lake study area, and 66.9 % in the Tustumena Lake study area between 1950–

372   ca. 2010. These changes equate to loss rates of 0.9 % yr^{-1} for Mystery Creek and 1.1 % yr^{-1} for

373   the Watson, Browns, and Tustumena Lake study areas (Table 3). Mean area loss for all four

374   sites was 0.8 % yr^{-1} between 1950 and 1984. During this time, loss rate was greatest for Watson

375   Lake and Brown Lake and least for Mystery Creek. Mean loss rate for all four sites increased to

376   2.3 % yr^{-1} between 1984 and 1996. During this time, loss rates were greatest in the north and

377   least in the south with Mystery Creek and Tustumena Lake losing 3.0 % yr^{-1} and 1.2 % yr^{-1},

378   respectively. Average loss rates decreased to 1.8 % yr^{-1} between 1996 and 2010, with the three

379   most northern sites losing approximately 1.2 % yr^{-1}, while the Tustumena Lake study area lost

380   3.2 % yr^{-1}. In terms of plateau area lost per year within the three time periods, Mystery Creek

381   (13.8 ha yr^{-1}), Watson Lake (1.6 ha yr^{-1}), and Browns Lake (1.3 ha yr^{-1}) experienced the greatest

382   areal loss rate during the 1984–1996 time period. At the Tustumena Lake study area, the greatest

383   rate of plateau extent loss (4.6 ha yr^{-1}) occurred between 1996–ca. 2010 (Table 3).

384   This study also assessed whether the permafrost degradation occurred along the perimeter

385   of the plateau (marginal), whether degradation was internal to the plateau, or if complete

386   degradation of a plateau occurred. Between 1950–2010, 85.0 % of the degradation occurred as

387   lateral thaw along the plateau margins, while internal thaw and complete loss of features

388   accounted for 1.5 % and 13.4 %, respectively. Lateral loss of permafrost was greatest in the

389   Watson Lake study area (90.9 %) and least (77.0 %) in the Browns Lake study area. Both

390   Mystery Creek and Tustumena Lake shared a lateral loss of 86.0 %. Mystery Creek saw the

391   greatest percent of internal collapse loss (3.3 %) compared to Tustumena (1.7 %) and Watson

392   and Browns Lake (both <1.0 %). The complete loss of permafrost features was greatest in

393   Browns Lake (22.4 %) and least in Watson Lake (8.3 %). Mystery Creek and Tustumena Lake

394   had 10.5 % and 12.3 %, respectively, of their permafrost plateaus disappear in the form of

395   complete feature loss. During the period of remotely sensed observations complete feature loss

396   increased from 6.7 % (1950–1984) to 21.0 % (1996–ca. 2010) of the detected change, while

397   lateral feature loss decreased from 91.0 % (1950–1984) to 78.1 % (1996–ca. 2010) of the

398   detected change, likely highlighting the role of fragmentation promoting complete feature

399   degradation.

400   **4.4 Climate and Weather Data**

401   The MAAT of the western Kenai Peninsula lowlands between 1981–2010 was 2.22 °C for the

402   KMA station and estimated to be 1.79 °C for the MRC station. There was significant correlation

403   between the KMA and MRC daily mean air temperatures for the 2012–2015 period (r^2=0.97).

404   The regression equation performed well during validation tests (r^2=0.95) and was therefore used

405   to estimate daily temperature data for the MRC station back to July 1948. Mean annual air

406   temperature has increased by 0.4 °C since 1950, with a step increase occurring in 1976

407   associated with the Pacific Decadal Oscillation (PDO) (Hartmann and Wendler, 2005) (Fig. 2).

408   Between July 1948 and December 1976, MAAT was 0.83 °C and 0.29°C for KMA and MRC,

409   respectively. Following the PDO shift MAAT increased to 1.97 °C and 1.51 °C for KMA and the

410   MRC, respectively (Fig. 2). Prior to the PDO shift, 18 (MRC) and 6 (KMA) out of 27 years had

411   a MAAT below freezing and after the PDO shift, only 10 (MRC) and 0 (KMA) out of 39 years

412   had a MAAT below freezing. MAAT at the MRC station was 0.88 °C (2012), 2.58 °C (2013),

413   and 3.24 °C (2014) during our three-year ground temperature observation period of 16

414   September 2012 to 15 September 2015. Therefore, the observations during 2014–2015 occurred

415   during a period with anomalously high MAAT relative to the previous climate normal period,

416   with more warming in the winter than the summer months (Table 1). Additionally, between

417   1948–2015, warm season (May-September) air temperatures increased by 0.02 °C yr^{-1} for both

418   the Kenai and MRC station, while winter season (October-April) air temperature increased by

419   0.04 °C yr^{-1} (Table 4).

420

5 Discussion

5.1 Presence of ecosystem-protected permafrost in southcentral Alaska

423   These permafrost data for the residual permafrost plateaus on the Kenai Peninsula are the first

424   such observations for isolated permafrost bodies in southcentral Alaska (Osterkamp, 2007).

425   Based on the five classes of permafrost proposed by Shur and Jorgenson (2007), the permafrost

426   present in wetland complexes of the western Kenai Peninsula lowlands is ecosystem-protected.

427   The permafrost on the Kenai Peninsula is extremely warm, with a MAGT that ranges from -0.04

428   to -0.08 °C (Table 1; Fig. 6). Permafrost ground temperatures at all monitoring sites were near

429   the phase-equilibrium temperature at depths from 1.0–3.0 m. Latent-heat effects associated with

430   unfrozen water content in permafrost and with seasonal phase changes in the active layer can

431   buffer the ground thermal regime from changes in air temperature at warm permafrost sites

432   (Romanovsky and Osterkamp, 2000) and in part can explain the persistence of ecosystem-

433   protected permafrost on the Kenai Peninsula (Shur and Jorgenson, 2007; Jorgenson et al., 2010).

434   Even though all thermistors were calibrated prior to installation, the ability to resolve such warm

435   permafrost temperatures and their change over time using temperature alone is somewhat

436   limiting. Thus, future measurements at the residual permafrost plateau sites in southcentral

437   Alaska will be accompanied by the addition of soil moisture probes as well as borehole, nuclear

438   magnetic resonance (NMR) which provides a direct measure of liquid water content (Parsekian

439   et al., 2013).

440   Field surveys that included probing, augering, coring and GPR provided additional

441   information on the vertical and spatial distribution of the warm permafrost on the western Kenai

442   Peninsula lowlands. The average active layer thickness at the permafrost plateau ground

443   temperature observation sites was 0.58 m. These sites were chosen for initial instrumentation in

444   September 2012 based in part on the relatively shallow depth to the frost table. More

445   comprehensive probing in September 2015 revealed that the average depth to the permafrost

446   table was 1.48 m (n=222) as averaged across three plateaus. At the Brown Lake plateau, a talik

447   overlying the permafrost table was present in February 2016. Average permafrost thickness at

448   this feature was 5.61 m thick, whereas at an adjacent feature it was more than 6.90 m, the

449   maximum depth of the auger flights. GPR survey data confirmed the presence of a continuous

450   surface talik at the Browns Lake site (Fig. 10); however, we were unable to image the base of the

451   permafrost using solely GPR, as similarly described by Lewkowicz et al. (2011). Based on visual

452   interpretation of the permafrost peat core acquired at the PF-BL-6 site in February 2016, the

453   permafrost deposit consists mainly of ice-rich frozen peat with well-developed organic-matrix

454   porphyritic and microlenticular cryostructures and some layered ice lenses, belt-like, and

455   suspended cryostructures (Fig. 8 and Fig. 9). Laboratory analysis also revealed gravimetric and

456   volumetric ice contents up to 1873 % and 96 %, respectively (Fig. 8).

457   **5.2 Extent and change in residual permafrost plateaus since the 1950s**

458   While previous reports of permafrost on the Kenai Peninsula exist (Hopkins et al., 1955;

459   Jorgenson et al., 2008), they were restricted to the wetland complex (Mystery Creek) north of

460   Sterling (Berg et al., 2009). Information on its dynamics here and elsewhere was lacking. The

461   analysis of remotely sensed imagery and field surveys identified residual permafrost plateaus in

462   three additional wetland complexes where it had not been previously identified (Fig. 1 and Fig.

463   11) and indicated that the state of permafrost within the Kenai lowlands is highly dynamic. In

464   1950, forested-permafrost plateau extent accounted for 19.0 % of the land cover in the 4,810 ha

465   of wetland complexes analysed in the four change detection study areas. In each of the wetland

466   areas analysed, permafrost plateaus accounted for more than 10.0 % of the area in 1950.

467   However, inferred permafrost extent decreased by 60.0 % between 1950–ca. 2010, and its lateral

468   coverage dropped below 5.0 % in three of the four study areas (Table 2).

469   The residual permafrost plateaus documented in this study share similar attributes to

470   features elsewhere in boreal peatlands for which permafrost degradation has been inferred due to

471   the ease of remotely detecting the conversion from forested permafrost plateau to non-permafrost

472   herbaceous wetland or waterbody (Jorgenson et al., 2001, 2008, 2012). Thie (1974) inferred a

473   permafrost plateau loss rate of 0.47 % yr^{-1} between 1800–1960 for a 130,000 ha area of southern

474   Manitoba. In Québec, Canada, a 13 ha peat bog lost 1.80 % yr^{-1} between 1957–2003 (Payette et

475   al., 2004). In the Northwest Territories, Canada, Quinton et al. (2011) reported a loss rate of

476   0.62 % yr^{-1} between 1947–2008 across a 100 ha study area. In Interior Alaska (Tanana Flats),

477   Jorgenson et al. (2001) reported a loss rate of 0.76 % yr^{-1} for birch forested permafrost plateaus

478   between 1949–1995 using a point sampling method within a 260,000 ha wetland area. Lara et al.

479   (2016) recently updated these numbers for the Tanana Flats by manually digitizing features with

480   methods similar to ours and demonstrated that birch forest plateaus decreased at a much slower

481   rate of 0.12 % yr^{-1}, and that black spruce forested permafrost plateau features appeared to be

482   stable. Thus, the loss rate of 1.0 % yr^{-1} that we report for the 4,810 ha mapped on the western

483   Kenai Peninsula Lowlands between 1950–ca. 2010 are the second fastest change rates reported

484   thus far in boreal peatlands.

5.3 Drivers of permafrost loss

Permafrost on the Kenai Peninsula is likely degrading as a result of warming air temperatures (+0.4 °C decade^{-1} since 1950), especially where warming during the winter season likely exacerbates these effects (Table 4). During the three-year observation period as well as since the 1950s, warming in the winter has been more pronounced than in the summer (Table 1 and Fig. 2) and 2014–2015 had a MAAT roughly double the 1981–2010 climate normal period. Storm systems regularly bring warm air masses (>4 °C) to the region during the winter. Air temperature warming during the winter months has decreased the number of freezing degree-days which means that the ground freezes to a much lesser degree in the winter (Fig. 2 and Table 1). Therefore, ground temperatures decreased less over the winter period (Fig. 5 and Table 1), potentially leading to talik development. Previous research on permafrost plateaus in colder regions indicate that preferential warming in the winter and increased snow accumulation leads to enhanced permafrost thaw in boreal peatlands (Camill, 2005; Osterkamp, 2007). Since the Kenai Peninsula lowlands experience a semi-continental climate due to the rain shadow produced by the Kenai Mountains, a lack of winter snowfall may have contributed to permafrost persistence in this region by allowing relatively cold winter air temperatures to propagate into the sub-surface. Thus, talik formation and permafrost degradation at the study sites in southcentral Alaska are likely being driven for the most part by winter air temperature warming (Fig. 2).

The increase in permafrost loss rate in southcentral Alaska following the 1980s is likely due to the combined effects of forest fires and a shift in the PDO after 1976. The respective pulse and press disturbances may have promoted large areas of permafrost already close to thawing, to quickly thaw, leaving only colder permafrost and permafrost with intact peat and forest cover. Fire can be an important driver of permafrost thaw (Yoshikawa et al., 2002) and

508 thermokarst development (Jones et al., 2015). The Kenai Fire of 1947 burned the majority of the

509 Mystery Creek study area, all of the Watson Lake study area, and the majority of the Browns

510 Lake study area. Evidence of this fire was seen at numerous sites in the Watson Lake and

511 Browns Lake study areas. Watson Lake and Browns Lake subsequently had the two greatest loss

512 rates between 1950–1984 which may be related to the 1947 fire. However, the presence of black

513 spruce burn poles were not found on all permafrost plateaus visited indicating that the burning

514 was likely relatively patchy in the wetlands. At Browns Lake, permafrost islands that did not

515 burn in 1947 exhibited less degradation, had thicker permafrost, denser tree cover, and larger

516 trees than the islands that burned. Large portions of the Tustumena Lake study area burned in

517 the 1996 Crooked Creek Fire and 2005 Fox Creek Fire. These fires likely damaged, and partially

518 removed the protective ecosystem cover (black spruce forest and peat), and degraded several

519 permafrost plateau features. This resulted in the Tustumena study area having the highest

520 change rate for the latter time period and 77.0 % of the plateau loss that occurred between 1996–

521 ca. 2010 did so in areas that burned in the 1996 and 2005 fires.

522   Bottom-up permafrost degradation was documented over the short period of direct

523 measurements between 2012–2015. The bottom-up permafrost thaw observed at the Watson

524 Lake PF2 site indicates that the flow of groundwater below the permafrost plateaus could be

525 responsible for degradation (Walters et al., 1998). In addition, analysis of the remotely sensed

526 imagery for the four select wetland complexes primarily documented lateral permafrost

527 degradation since the 1950s, as inferred by the conversion of forested plateau margins to

528 herbaceous wetland vegetation. This type of feature loss accounted for 85.0% of the change

529 between 1950–ca. 2010. This pattern of loss was further observed in the field through the

530 presence of thermokarst moats and drowning black spruce trees along the margins of the

531 permafrost plateaus (Fig. 3). This is similar to the dominant processes documented in more

532 northerly boreal peatlands with permafrost plateaus (Thie, 1974; Camill and Clark, 1998;

533 Osterkamp et al., 2000; Jorgenson et al., 2001; Payette et al., 2004; Quinton et al., 2011;

534 Jorgenson et al., 2012; O'Donnell et al., 2012; Lara et al., 2015). These findings highlight the

535 importance of groundwater flow and also the impact of saturated herbaceous wetlands that

536 absorb heat during the summer that likely degrades permafrost along the peat plateau margins

537 (Walters et al., 1998). It is possible that lateral permafrost degradation caused by these processes

538 is overwhelming the protection provided by the ecosystem cover for permafrost stability on the

539 Kenai Peninsula lowlands. Future research is required to more fully understand the role of

540 groundwater movement on permafrost instability in the study region.

541 **5.4 Proposed history of permafrost on the Kenai Peninsula**

542 During the Last Glacial Maximum (LGM), northern hemisphere permafrost extended much

543 further south than present day (Lindgren et al., 2015). However, permafrost history in

544 southcentral Alaska is poorly constrained. Even though the western Kenai Peninsula lowlands

545 were almost completely glaciated during the LGM (Reger et al., 2007), the permafrost features

546 identified in this study occur in glaciolacustrine or glaciofluvial wetland complexes that were

547 either not glaciated during the LGM (Mystery Creek) or became deglaciated before

548 16,000 cal yrs BP (Reger et al., 2007). Perhaps permafrost formed on the Kenai Peninsula

549 during deglaciation or shortly thereafter during the Younger Dryas 12,900–11,700 years ago

550 (Jones et al., 2009). However, this permafrost would have likely thawed during the Holocene

551 Thermal Maximum (Zoltai, 1972; Kaufman et al., 2004). As the regional climate became cooler

552 and wetter, between 8,000–5,000 years ago, *Sphagnum* accumulation and preservation on the

553 western Kenai Peninsula lowlands may have promoted more widespread permafrost aggradation

554 (Jones et al., 2009). Following this period, the peatlands may have progressively froze, heaving

555 the permafrost plateaus above the water table, drying the peat-rich soils, promoting growth of

556 black spruce, and creating a buffer layer protecting the underlying permafrost (ecosystem-

557 protected) from the unfavourable climate for permafrost that currently exists today (Zoltai, 1972,

558 1995; Payette et al., 2004; Camill, 2005; Shur and Jorgenson, 2007). Growth of permafrost and

559 heaving the peatland surface above the water table could explain low peat accumulation rates

560 calculated in many Kenai Peninsula peatlands between 3,300–2,000 years ago (Jones and Yu,

561 2010; Jones et al., 2014). This also coincides with widespread neoglaciation on the Kenai

562 Peninsula 3,000–1,500 years ago (Wiles and Calkin, 1994, Barclay et al., 2009). Alternatively,

563 the Little Ice Age (365–165 years ago), promoted shallow permafrost formation in areas that

564 were predominantly unfrozen throughout the Holocene (Romanovsky et al., 1992; Jorgenson et

565 al., 2001), and thus, could account for the presence of residual permafrost on the Kenai

566 Peninsula. The widespread loss of permafrost plateaus in central Alaska may be a result of

567 degradation of Little Ice Age permafrost (Jorgenson et al., 2001). The age, history, and future

568 trajectory of permafrost on the western Kenai Peninsula lowlands require further study.

569 **5.5 Landscape dynamics and permafrost thaw on the western Kenai Peninsula lowlands**

570 Previous and ongoing land cover change on the western Kenai Peninsula lowlands are primarily

571 in response to the interaction of climate change and human development. Increases in summer

572 air temperature and late-summer droughts, along with human disturbance, have been linked to

573 the massive spruce bark beetle (*Dendroctonus rufipennis*) outbreak of the late 1990s (Berg et al.,

574 2006; Sherriff et al., 2011), which led to subsequent timber salvage (Jones, 2008). Berg and

575 Anderson (2006) caution that overall drier conditions on the western Kenai Peninsula, combined

576 with standing dead spruce stands, may alter the future fire regime of this region. Wetland drying

577   (Klein et al., 2005) and establishment of woody vegetation in wetlands (Berg et al., 2009) may

578   be attributed to warmer air temperatures and decreases in precipitation. Furthermore, tectonic

579   activity associated with the Great Alaska Earthquake of 1964 caused the western Kenai

580   Peninsula to lower in elevation by 0.7–2.3 m (Plafker, 1969), while the northern portion of the

581   peninsula subsequently uplifted 0.8–0.9m (Cohen and Freymueller, 1997), potentially altering

582   groundwater flow paths (Gracz, 2011).

583   In this study, the loss of ecosystem-protected permafrost in the overall understanding of

584   landscape dynamics on the western Kenai Peninsula lowlands was documented and incorporated.

585   The degradation of permafrost can impact terrestrial and aquatic ecosystems, hydrology,

586   infrastructure, and carbon cycling on the Kenai Peninsula (Schuur et al., 2008; Grosse et al.,

587   2011; Jorgenson et al., 2013; Kokelj et al., 2015; Vonk et al., 2015). Permafrost degradation

588   within the wetlands is responsible for a shift from black spruce forest plateaus to fen and bog

589   wetland ecosystems at a mean rate of 9.2ha yr^{-1} since the 1950s in the four change detection

590   study areas. Permafrost plateaus redirect surface and near-surface drainage in boreal wetlands

591   (Quinton et al., 2011), and the thaw subsidence of these features increases drainage network

592   connectivity (Beilman and Robinson, 2003), and alters the local hydrological cycle (Hayashi et

593   al., 2007). Thus, the loss of permafrost and/or changes in seasonally frozen ground phenology

594   could in part be aiding in observations of terrestrial and aquatic changes that have occurred on

595   the Kenai Peninsula during the past several decades. Further work is required to better

596   understand the past influence of permafrost on the Kenai Peninsula as well as the future loss of

597   these warm permafrost deposits.

6 Conclusions

Based on the ground data and remotely sensed observations, it was found that peatland permafrost is currently more extensive than previously reported in southcentral Alaska, a region with a MAAT of 1.5 °C. Warm permafrost (-0.04 °C to -0.08 °C) persists on the western Kenai Peninsula lowlands in forested (black spruce), peat plateaus found in glaciolacustrine and glaciofluvial wetland complexes. At the field study sites, the depth to permafrost table on the peat plateaus averaged 1.48 m in September 2015, but was as shallow as 0.53 m at some locations. Permafrost thickness ranged from 0.33 m to greater than 6.90 m. Field surveys conducted in February 2016 documented the presence of a surface talik overlying the permafrost table. In 1950, residual permafrost plateaus covered 19.0 % of the 4,810 ha wetland area mapped in the study. Within the changed detection study areas, 60.0 % of the permafrost plateaus present in 1950 had degraded by ca. 2010. In most cases, permafrost degradation equated to the loss of forest and its replacement by bog or fen vegetation, preferentially occurring along permafrost plateau margins. Permafrost loss on the Kenai Peninsula is likely associated with a warming climate, particularly during the winter season, wildfires that remove the protective ecosystem cover, groundwater flow at depth, and lateral heat transfer from wetland surface waters in the summer. Future studies on the residual permafrost plateaus on the Kenai Peninsula will provide further insight for mapping and predicting permafrost extent across Boreal permafrost regions that are currently warming.

7 Data availability

All data available upon request to the corresponding author.

8 Author contribution

B.M. Jones devised the study design and prepared the manuscript with contributions from all co-authors. B.M. Jones, C.A. Baughman, V.E. Romanovsky, E.L. Babcock, A.D. Parsekian, M.C. Jones, and E.E. Berg contributed to field instrumentation and field studies. B.M. Jones, C.A. Baughman, and G. Grosse conducted and contributed to remote sensing analysis. C.A. Baughman compiled and interpolated regional weather and climate station data. E.Stephani conducted the cryofacies analysis and laboratory testing. All co-authors contributed substantially to this research.

9 Acknowledgements

10 References

Allard M., Seguin M. K., and Levesque R.: Palsas and mineral permafrost mounds in northern Quebec, In International Geomorphology, Part II, Gardiner V (ed). John Wiley and Sons Ltd: Chichester; 285–309, 1986.

640 Anderson, R. S., Hallett, D. J., Berg, E., Jass, R. B., Toney, J. L., Fontaine, C. S. de and
641   DeVolder, A.: Holocene development of Boreal forests and fire regimes on the Kenai
642   Lowlands of Alaska, The Holocene, 16(6), 791–803, doi:10.1191/0959683606hol966rp,
643   2006.

644 Barclay, D.J., Wiles, G.C. and Calkin, P.E.: Holocene glacier fluctuations in Alaska. Quaternary
645   Science Reviews, 28, 2034-2048, 2009.

646 Beilman, D. W. and Robinson, S. D.: Peatland permafrost thaw and landform type along a
647   climatic gradient, Proc 8th Int Conf Permafr. Zurich Switz. 21–25 July 2003, 61 – 65, 2003.

648 Beilman, D. W., Vitt, D. H. and Halsey, L. A.: Localized Permafrost Peatlands in Western
649   Canada: Definition, Distributions, and Degradation, Arct. Antarct. Alp. Res., 33(1), 70–77,
650   doi:10.2307/1552279, 2001.

651 Berg, E. E. and Anderson, R. S.: Fire history of white and Lutz spruce forests on the Kenai
652   Peninsula, Alaska, over the last two millennia as determined from soil charcoal, For. Ecol.
653   Manag., 227(3), 275–283, doi:10.1016/j.foreco.2006.02.042, 2006.

654 Berg, E. E., David Henry, J., Fastie, C. L., De Volder, A. D. and Matsuoka, S. M.: Spruce beetle
655   outbreaks on the Kenai Peninsula, Alaska, and Kluane National Park and Reserve, Yukon
656   Territory: Relationship to summer temperatures and regional differences in disturbance
657   regimes, For. Ecol. Manag., 227(3), 219–232, doi:10.1016/j.foreco.2006.02.038, 2006.

658 Berg, E. E., Hillman, K. M., Dial, R. and DeRuwe, A.: Recent woody invasion of wetlands on
659   the Kenai Peninsula Lowlands, south-central Alaska: a major regime shift after 18 000 years
660   of wet Sphagnum–sedge peat recruitment, Can. J. For. Res., 39(11), 2033–2046,
661   doi:10.1139/X09-121, 2009.

662 Brown, J., Ferrians, O. J., Heginbottom, J. A. and Melnikov, E. S.: Circum-Arctic Map of
663   Permafrost and Ground Ice Conditions, 1998.

664 Brown, R. J. E.: The Distribution of Permafrost and Its Relation to Air Temperature in Canada
665   and the U.S.S.R., ARCTIC, 13(3), 163–177, doi:10.14430/arctic3697, 1960.

666 Brown, R. J. E.: Permafrost in Canada: its influence on Northern development, University of
667   Toronto Press., 1970.

668 Cable, W. L., Romanovsky, V. E., and Jorgenson, M. T.: Scaling-up permafrost thermal
669   measurements in western Alaska using an ecotype approach, The Cryosphere, 10, 2517-
670   2532, doi:10.5194/tc-10-2517-2016, 2016.

671 Camill, P.: Patterns of boreal permafrost peatland vegetation across environmental gradients
672   sensitive to climate warming, Can. J. Bot., 77(5), 721–733, doi:10.1139/b99-008, 1999.

673 Camill, P.: Permafrost Thaw Accelerates in Boreal Peatlands During Late-20th Century Climate
674   Warming, Clim. Change, 68(1–2), 135–152, doi:10.1007/s10584-005-4785-y, 2005.

675 Camill, P. and Clark, J. S.: Climate Change Disequilibrium of Boreal Permafrost Peatlands
676   Caused by Local Processes, Am. Nat., 151(3), 207–222, doi: 10.1086/286112, 1998.

677 Cohen, S.C. and Freymueller, J.T.: Deformation of the Kenai Peninsula, Alaska, Journal of
678   Geophysical Research: Solid Earth, 102, 20479-20487. 1997.

679 Ferrians, O. J.: Permafrost Map of Alaska, U.S. Geological Survey Miscellaneous Geologic
680   Investigations Map I-445, scale 1:2,500,000, 1965.

681 Gooseff, M. N., Balser, A., Bowden, W. B. and Jones, J. B.: Effects of Hillslope Thermokarst in
682   Northern   Alaska,   Eos   Trans.   Am.   Geophys.   Union,   90(4),   29–30,
683   doi:10.1029/2009EO040001, 2009.

684 Gracz, M. B.: Comment on "Wetland drying and succession across the Kenai Peninsula
685   Lowlands, south-central Alaska" Appears in Can. J. For. Res. 35: 1931-1941 (2005)., Can.
686   J. For. Res., 41(2), 425–428, doi:10.1139/X10-147, 2011.

687 Grosse, G., Harden, J., Turetsky, M., McGuire, A. D., Camill, P., Tarnocai, C., Frolking, S.,
688   Schuur, E. A. G., Jorgenson, T., Marchenko, S., Romanovsky, V., Wickland, K. P., French,
689   N., Waldrop, M., Bourgeau-Chavez, L. and Striegl, R. G.: Vulnerability of high-latitude soil
690   organic carbon in North America to disturbance, J. Geophys. Res. Biogeosciences, 116(G4),
691   G00K06, doi:10.1029/2010JG001507, 2011.

692 Hartmann, B., and Wendler, G.: The significance of the 1976 Pacific climate shift in the
693   climatology of Alaska, Journal of Climate, 18(22), 4824–4839, 2005.

694 Hayashi, M., Goeller, N., Quinton, W. L. and Wright, N.: A simple heat-conduction method for
695   simulating the frost-table depth in hydrological models, Hydrol. Process., 21(19), 2610–
696   2622, doi:10.1002/hyp.6792, 2007.

697 Hopkins, D. M., Karlstrom, T. N. V., others, others and others: Permafrost and Ground Water in
698   Alaska, Geological Survey Professional Paper, U.S. Geological Survey, United States
699   Government Printing Office., 1955.

700 Jafarov, E. E., Romanovsky, V. E., Genet, H., McGuire, A. D. and Marchenko, S. S.: The effects
701   of fire on the thermal stability of permafrost in lowland and upland black spruce forests of

interior Alaska in a changing climate, Environ. Res. Lett., 8(3), 035030, doi:10.1088/1748-9326/8/3/035030, 2013.

Jones, B. M.: Land-cover change on the southern Kenai Peninsula lowlands, Alaska using USGS land cover trends methodology, J. Geogr. Reg. Plan., 1(4), 068–071, 2008.

Jones, B. M., Grosse, G., Arp, C. D., Miller, E., Liu, L., Hayes, D. J. and Larsen, C. F.: Recent Arctic tundra fire initiates widespread thermokarst development, Sci. Rep., 5, doi:10.1038/srep15865, 2015.

Jones, M. C., Peteet, D. M., Kurdyla, D. and Guilderson, T.: Climate and vegetation history from a 14,000-year peatland record, Kenai Peninsula, Alaska, Quat. Res., 72(2), 207–217, doi:10.1016/j.yqres.2009.04.002, 2009.

Jones, M.C. and Yu, Z.: Rapid deglacial and early Holocene expansion of peatlands in Alaska, Proceedings of the National Academy of Sciences, 107, 7347-7352, 2010.

Jones, M.C., Wooller, M. and Peteet, D.M.: A deglacial and Holocene record of climate variability in south-central Alaska from stable oxygen isotopes and plant macrofossils in peat, Quaternary Science Reviews, 87, 1–11, 2014.

Jorgenson, M. T., Racine, C. H., Walters, J. C. and Osterkamp, T. E.: Permafrost Degradation and Ecological Changes Associated with a Warming Climate in Central Alaska, Clim. Change, 48(4), 551–579, doi:10.1023/A:1005667424292, 2001.

Jorgenson, M. T. and Osterkamp, T. E.: Response of boreal ecosystems to varying modes of permafrost degradation, Can. J. For. Res., 35(9), 2100–2111, doi:10.1139/x05-153, 2005.

Jorgenson, M.T., Roth, J.E., Schlentner, S.F., Pullman, E.R. and Macander, M.: An ecological land survey for Fort Richardson, Alaska (No. ERDC/CRREL-TR-03-19). Engineer Research And Development Center Hanover Cold Regions Research And Engineering Lab, 2003.

Jorgenson, M. T., Shur, Y. L. and Pullman, E. R.: Abrupt increase in permafrost degradation in Arctic Alaska, Geophys. Res. Lett., 33(2), L02503, doi:10.1029/2005GL024960, 2006.

Jorgenson, T., Shur, Y.L., Osterkamp, T.E.: Thermokarst in Alaska. In Proceedings of the Ninth International Conference on Permafrost, Vol. 1, June 29–July 3, 2008, Fairbanks, Alaska, Kane DL, Hinkel KM (eds). Institute of Northern Engineering, University of Alaska Fairbanks; 869–876, 2008.

Jorgenson, M. T., Yoshikawa, K., Kanevskiy, M. Z., Shur, Y., Romanovsky, V. E., Marchenko, S., Grosse, G., Brown, J. and Jones, B. M.: Permafrost characteristics of Alaska, in 9th International Conference on Permafrost, 2008.

Jorgenson, M. T., Romanovsky, V., Harden, J., Shur, Y., O'Donnell, J., Schuur, E. A. G., Kanevskiy, M. and Marchenko, S.: Resilience and vulnerability of permafrost to climate change, Can. J. For. Res., 40(7), 1219–1236, doi:10.1139/X10-060, 2010.

Jorgenson, M.T., Kanevskiy, M., Shur, Y., Osterkamp, T., Fortier, D., Cater, T., Miller, P.: Thermokarst lake and shore fen development in boreal Alaska. In Proceedings of the Tenth International Conference on Permafrost, Vol. 1 International contributions, June 25–29, 2012, Salekhard, Russia, Hinkel KM (ed.). The Northern Publisher: Salekhard, Russia; 179–184, 2012.

Jorgenson, M. T., Harden, J., Kanevskiy, M., O'Donnell, J., Wickland, K., Stephanie Ewing, Manies, K., Zhuang, Q., Shur, Y., Striegl, R. and Koch, J.: Reorganization of vegetation, hydrology and soil carbon after permafrost degradation across heterogeneous boreal landscapes, Environ. Res. Lett., 8(3), 035017, doi:10.1088/1748-9326/8/3/035017, 2013.

Kanevskiy, M., Jorgenson, T., Shur, Y., O'Donnell, J.A., Harden, J.W., Zhuang, Q., and Fortier, D.: Cryostratigraphy and Permafrost Evolution in the Lacustrine Lowlands of West-Central Alaska, Permafrost and Periglacial Processes, 25(1), 14-34, 2014.

Kanevskiy, M., Shur, Y., Krzewinski, T. and Dillon, M.: Structure and properties of ice-rich permafrost near Anchorage, Alaska, Cold Reg. Sci. Technol., 93, 1–11, doi:10.1016/j.coldregions.2013.05.001, 2013.

Kaufman, D.S., Ager, T.A., Anderson, N.J., Anderson, P.M., Andrews, J.T., Bartlein, P.J., Brubaker, L.B., Coats, L.L., Cwynar, L.C., Duvall, M.L. and Dyke, A.S.: Holocene thermal maximum in the western Arctic (0–180 W). Quaternary Science Reviews, 23, 529–560, 2004.

Klein, E., Berg, E. E. and Dial, R.: Wetland drying and succession across the Kenai Peninsula Lowlands, south-central Alaska, Can. J. For. Res., 35(8), 1931–1941, doi:10.1139/x05-129, 2005.

Kokelj, S. V., Tunnicliffe, J., Lacelle, D., Lantz, T. C., Chin, K. S. and Fraser, R.: Increased precipitation drives mega slump development and destabilization of ice-rich permafrost

terrain, northwestern Canada, Glob. Planet. Change, 129, 56–68, doi:10.1016/j.gloplacha.2015.02.008, 2015.

Lachenbruch, A. H. and Marshall, B. V.: Changing Climate: Geothermal Evidence from Permafrost in the Alaskan Arctic, Science, 234(4777), 689–696, doi:10.1126/science.234.4777.689, 1986.

Lantz, T. C. and Kokelj, S. V.: Increasing rates of retrogressive thaw slump activity in the Mackenzie Delta region, N.W.T., Canada, Geophys. Res. Lett., 35(6), L06502, doi:10.1029/2007GL032433, 2008.

Lara, M. J., Genet, H., McGuire, A. D., Euskirchen, E. S., Zhang, Y., Brown, D. R. N., Jorgenson, M. T., Romanovsky, V., Breen, A. and Bolton, W. R.: Thermokarst rates intensify due to climate change and forest fragmentation in an Alaskan boreal forest lowland, Glob. Change Biol., doi:10.1111/gcb.13124, 2015.

Lewkowicz, A.G., Etzelmüller, B. and Smith, S.L.: Characteristics of discontinuous permafrost based on ground temperature measurements and electrical resistivity tomography, southern Yukon, Canada, Permafrost and Periglacial Processes, 22(4), pp.320-342, 2011.

Liljedahl, A.K., Boike, J., Daanen, R.P., Fedorov, A.N., Frost, G.V., Grosse, G., Hinzman, L.D., Iijma, Y., Jorgenson, J.C., Matveyeva, N., Necsoiu, M., , Raynolds, M. K., Romanovsky, V. E., Schulla, J., Tape, K., Walker, D. A., and H. Yabuki: Pan-Arctic ice-wedge degradation in warming permafrost and its influence on tundra hydrology, Nature Geoscience, 2016.

Lindgren, A., Hugelius, G., Kuhry, P., Christensen, T. R. and Vandenberghe, J.: GIS-based Maps and Area Estimates of Northern Hemisphere Permafrost Extent during the Last Glacial Maximum, Permafr. Periglac. Process., n/a–n/a, doi:10.1002/ppp.1851, 2015.

Lunardini, V.J.: Climatic warming and the degradation of warm permafrost. Permafrost and Periglacial Processes, 7(4), 311-320, 1996.

Lynch, J. A., Clark, J. S., Bigelow, N. H., Edwards, M. E. and Finney, B. P.: Geographic and temporal variations in fire history in boreal ecosystems of Alaska, J. Geophys. Res. Atmospheres, 107(D1), 8152, doi:10.1029/2001JD000332, 2002.

Morse, P. D., Wolfe, S. A., Kokelj, S. V. and Gaanderse, A. J. R.: The Occurrence and Thermal Disequilibrium State of Permafrost in Forest Ecotopes of the Great Slave Region, Northwest Territories, Canada, Permafr. Periglac. Process., doi:10.1002/ppp.1858, 2015.

792 Murton, J.B, and French, H.M.: Cryostructures in permafrost, Tuktoyaktuk coastlands, western
793 Arctic Canada. Canadian Journal of Earth Sciences, 31, pp.737–747, 1994.

794 Neal, A.: Ground-penetrating radar and its use in sedimentology: principles, problems and
795 progress, Earth-science reviews, 66, 261-330, 2004.

796 Nelson, F. E., Anisimov, O. A. and Shiklomanov, N. I.: Subsidence risk from thawing
797 permafrost, Nature, 410(6831), 889–890, doi:10.1038/35073746, 2001.

798 O'Donnell, J.A., Harden, J.W., McGuire, A.D., Kanevskiy, M.Z., Jorgenson, M.T., Xu, X. The
799 effect of fire and permafrost interactions on soil carbon accumulation in an upland black
800 spruce ecosystem of interior Alaska: implications for post-thaw carbon loss. Global Change
801 Biology 17: 1461–1474. DOI: 10.1111/j.1365-2486. 2010.02358, 2011.

802 O'Donnell, J. A., Jorgenson, M. T., Harden, J. W., McGuire, A. D., Kanevskiy, M. Z. and
803 Wickland, K. P.: The Effects of Permafrost Thaw on Soil Hydrologic, Thermal, and Carbon
804 Dynamics in an Alaskan Peatland, Ecosystems, 15(2), 213–229, doi:10.1007/s10021-011-
805 9504-0, 2012.

806 Osterkamp, T. E.: Characteristics of the recent warming of permafrost in Alaska, J. Geophys.
807 Res. Earth Surf., 112(F2), F02S02, doi:10.1029/2006JF000578, 2007.

808 Osterkamp, T. E., Viereck, L., Shur, Y., Jorgenson, M. T., Racine, C., Doyle, A. and Boone, R.
809 D.: Observations of Thermokarst and Its Impact on Boreal Forests in Alaska, U.S.A., Arct.
810 Antarct. Alp. Res., 32(3), 303–315, doi:10.2307/1552529, 2000.

811 Parsekian, A. D., Slater, L., Comas, X., and Glaser, P. H.: Variations in free-phase gases in peat
812 landforms determined by ground-penetrating radar, Journal of Geophysical Research:
813 Biogeosciences, 115, no. G2, 2010.

814 Parsekian, A.D., Grosse, G., Walbrecker, J.O., Müller-Petke, M., Keating, K., Liu, L., Jones,
815 B.M. and Knight, R.: Detecting unfrozen sediments below thermokarst lakes with surface
816 nuclear magnetic resonance, Geophysical Research Letters, 40(3), 535-540, 2013.

817 Pastick, N. J., Jorgenson, M. T., Wylie, B. K., Nield, S. J., Johnson, K. D. and Finley, A. O.:
818 Distribution of near-surface permafrost in Alaska: Estimates of present and future
819 conditions, Remote Sens. Environ., 168, 301–315, doi:10.1016/j.rse.2015.07.019, 2015.

820 Payette, S., Delwaide, A., Caccianiga, M. and Beauchemin, M.: Accelerated thawing of subarctic
821 peatland permafrost over the last 50 years, Geophys. Res. Lett., 31(18), L18208,
822 doi:10.1029/2004GL020358, 2004.

823   Plafker, G.: Tectonics of the March 27, 1964 Alaska earthquake: U.S. Geological Survey
824   Professional Paper. [online] Available from: http://pubs.usgs.gov/pp/0543i/, 1969.

825   Quinton, W. l., Hayashi, M. and Chasmer, L. e.: Permafrost-thaw-induced land-cover change in
826   the Canadian subarctic: implications for water resources, Hydrol. Process., 25(1), 152–158,
827   doi:10.1002/hyp.7894, 2011.

828   Reger, R. D., Sturmann, A. G., Berg, E. E. and Burns, P. A. C.: A guide to the late Quaternary
829   history of northern and western Kenai Peninsula, Alaska: Alaska Division of Geological &
830   Geophysical Surveys Guidebook 8, 2007.

831   Riddle, C.H., Rooney, J.W.: Encounters with relict permafrost in the Anchor- age, Alaska, area.
832   Proceedings of the Tenth International Conference on Permafrost, Salekhard, Yamal-Nenets
833   Autonomous District, Russia, June 25–29, 2012, 1, pp. 323–328, 2012.

834   Romanovsky, V. E., Garagula, L. S., and Seregina, N. V.: Freezing and thawing of soils under
835   the influence of 300- and 90-year periods of temperature fluctuation. Pages 543–548 in
836   Proceedings of the International Conference on the Role of Polar Regions in Global Change.
837   Fairbanks (AK): Geophysical Institute, University of Alaska. 1992.

838   Romanovsky, V. E. and Osterkamp, T. E.: Effects of unfrozen water on heat and mass transport
839   processes in the active layer and permafrost, Permafr. Periglac. Process., 11(3), 219–239,
840   doi:10.1002/1099-1530(200007/09)11:3<219::AID-PPP352>3.0.CO;2-7, 2000.

841   Romanovsky, V. E. and Osterkamp, T. E. (1995), Interannual variations of the thermal regime of
842   the active layer and near-surface permafrost in northern Alaska. Permafrost Periglac.
843   Process., 6: 313–335. doi: 10.1002/ppp.3430060404

844   Romanovsky, V., Burgess, M., Smith, S., Yoshikawa, K. and Brown, J.: Permafrost temperature
845   records: Indicators of climate change, Eos Trans. Am. Geophys. Union, 83(50), 589–594,
846   doi:10.1029/2002EO000402, 2002.

847   Romanovsky, V. E., Smith, S. L. and Christiansen, H. H.: Permafrost thermal state in the polar
848   Northern Hemisphere during the international polar year 2007–2009: a synthesis, Permafr.
849   Periglac. Process., 21(2), 106–116, doi:10.1002/ppp.689, 2010.

850   Sandmeier, K. J.: REFLEXW – WindowsTM 9x/NT/2000/XP-program for the processing of
851   seismic, acoustic or electromagnetic reflection, refraction and transmission data, 2008.

852   Sannel, A.B.K., Kuhry, P. : Long-term stability of permafrost in subarctic peat plateaus, west-
853   central Canada. The Holocene 18, 589–601, 2008.

854 Sannel, A.B.K., Kuhry, P.: Warming induced destabilization of peat plateau/thermokarst lake
855   complexes. Journal of Geophysical Research 116, G03035, doi:10.1029/2010JG001635,
856   2011.

857 Sannel, A. B. K., Hugelius, G., Jansson, P. and Kuhry, P.: Permafrost Warming in a Subarctic
858   Peatland – Which Meteorological Controls are Most Important?, Permafr. Periglac.
859   Process., n/a–n/a, doi:10.1002/ppp.1862, 2015.

860 Schuur, E. A. G., Bockheim, J., Canadell, J. G., Euskirchen, E., Field, C. B., Goryachkin, S. V.,
861   Hagemann, S., Kuhry, P., Lafleur, P. M., Lee, H., Mazhitova, G., Nelson, F. E., Rinke, A.,
862   Romanovsky, V. E., Shiklomanov, N., Tarnocai, C., Venevsky, S., Vogel, J. G. and Zimov,
863   S. A.: Vulnerability of Permafrost Carbon to Climate Change: Implications for the Global
864   Carbon Cycle, BioScience, 58(8), 701–714, doi:10.1641/B580807, 2008.

865 Sherriff, R. L., Berg, E. E. and Miller, A. E.: Climate variability and spruce beetle
866   (Dendroctonus rufipennis) outbreaks in south-central and southwest Alaska, Ecology, 92(7),
867   1459–1470, doi:10.1890/10-1118.1, 2011.

868 Shur, Y. L. and Jorgenson, M. T.: Patterns of permafrost formation and degradation in relation to
869   climate and ecosystems, Permafr. Periglac. Process., 18(1), 7–19, doi:10.1002/ppp.582,
870   2007.

871 Smith, M. W. and Riseborough, D. W.: Climate and the limits of permafrost: a zonal analysis,
872   Permafr. Periglac. Process., 13(1), 1–15, doi:10.1002/ppp.410, 2002.

873 Swindles, G.T., Morris, P.J., Mullan, D., Watson, E.J., Turner, T.E., Roland, T.P., Amesbury,
874   M.J., Kokfelt, U., Schoning, K., Pratte, S. and Gallego-Sala, A.: The long-term fate of
875   permafrost peatlands under rapid climate warming, Scientific Reports, 5, 17951,
876   10.1038/srep17951, 2015.

877 Thie, J.: Distribution and Thawing of Permafrost in the Southern Part of the Discontinuous
878   Permafrost Zone in Manitoba, ARCTIC, 27(3), 1974.

879 Turetsky, M. R., Wieder, R. K., Vitt, D. H., Evans, R. J. and Scott, K. D.: The disappearance of
880   relict permafrost in boreal North America: Effects on peatland carbon storage and fluxes,
881   Glob. Change Biol., 13(9), 1922–1934, doi:10.1111/j.1365-2486.2007.01381.x, 2007.

882 Van Everdingen, R. O.,: Multi-Language Glossary of Permafrost and Related Ground-Ice Terms
883   in Chinese, English, French, German, Icelandic, Italian, Norwegian, Polish, Romanian,

884   Russian, Spanish, and Swedish. International Permafrost Association, Terminology
885   Working Group, 1998.

886   Vonk, J. E., Tank, S. E., Bowden, W. B., Laurion, I., Vincent, W. F., Alekseychik, P., Amyot,
887   M., Billet, M. F., Canário, J., Cory, R. M., Deshpande, B. N., Helbig, M., Jammet, M.,
888   Karlsson, J., Larouche, J., MacMillan, G., Rautio, M., Walter Anthony, K. M. and
889   Wickland, K. P.: Reviews and syntheses: Effects of permafrost thaw on Arctic aquatic
890   ecosystems, Biogeosciences, 12(23), 7129–7167, doi:10.5194/bg-12-7129-2015, 2015.

891   Walters J.C., Racine C.H., and Jorgenson M.T.: Characteristics of permafrost in the Tanana
892   Flats, interior Alaska, In: Proceedings of the Seventh International Conference on
893   Permafrost Vol 57 (eds. Lewkowicz AG, Allard M), Université Laval, Québec. Collection
894   Nordicana, 1109–1116, 1998.

895   Wiles, G. C. and Calkin, P. E.: Late Holocene, high-resolution glacial chronologies and climate,
896   Kenai Mountains, Alaska, Geol. Soc. Am. Bull., 106(2), 281–303, doi:10.1130/0016-
897   7606(1994)106<0281:LHHRGC>2.3.CO;2, 1994.

898   Yoshikawa, K., Bolton, W. R., Romanovsky, V. E., Fukuda, M. and Hinzman, L. D.: Impacts of
899   wildfire on the permafrost in the boreal forests of Interior Alaska, J. Geophys. Res.
900   Atmospheres, 107(D1), 8148, doi:10.1029/2001JD000438, 2002.

901   Zoltai, S. C.: Palsas and Peat Plateaus in Central Manitoba and Saskatchewan, Can. J. For. Res.,
902   2(3), 291–302, doi:10.1139/x72-046, 1972.

903   Zoltai, S.C.: Cyclic development of permafrost in the peatlands of northwestern Alberta, Canada.
904   Arctic and Alpine Research 25, 240–246, 1993.

905   Zoltai, S. C.: Permafrost Distribution in Peatlands of West-Central Canada During the Holocene
906   Warm Period 6000 Years BP, Géographie Phys. Quat., 49(1), 45, doi:10.7202/033029ar,
907   1995.

removed
Tables

Table 1. Mean annual ground temperature (MAGT) data for four observation sites on the Kenai Peninsula lowlands. Browns Lake PF1, Watson Lake PF1, and Watson Lake PF2 represent permafrost plateaus and the Watson Lake non-PF site a black spruce forested non-plateau site. Sensor depths that were perennially frozen in a given year are in bold. Mean annual air temperature (MAAT), thawing and freezing degree days (TDD and FDD), and average winter snow depth (MASD) are from the he MRC station (Kenai 29 ENE - AWS 702590).

9/16/2012 - 9/15/2013

Browns Lake PF1		Watson Lake PF1		Watson Lake PF2		Watson Lake non-PF		KENAI 29 ENE AWS 702590 Met Station Data			
Sensor depth (cm)	MAGT (°C)	Sensor depth (cm)	MAGT (°C)	Sensor depth (cm)	MAGT (°C)	Sensor depth (cm)	MAGT (°C)	MAAT (°C)	TDD Sums	FDD Sums	MASD (cm)
50	-0.02	10	0.34	10	0.05	25	0.94				
100	**-0.06**	25	-0.09	50	-0.30	50	0.42	0.88	1865.9	1544.3	19.3
200	**-0.08**	50	-0.20	**100**	**-0.08**	100	0.14				
300	**-0.08**	**100**	**-0.08**	**200**	**-0.06**	130	0.16				

9/16/2013 - 9/15/2014

Browns Lake PF1		Watson Lake PF1		Watson Lake PF2		Watson Lake non-PF		KENAI 29 ENE AWS 702590 Met Station Data			
Sensor depth (cm)	MAGT (°C)	Sensor depth (cm)	MAGT (°C)	Sensor depth (cm)	MAGT (°C)	Sensor depth (cm)	MAGT (°C)	MAAT (°C)	TDD Sums	FDD Sums	MASD (cm)
50*	0.17	10	0.93	10	0.86	25	0.57				
100	**-0.06**	25	0.40	50	-0.07	50	0.32	2.58	2066.6	1123.4	8.3
200	**-0.06**	50	-0.02	**100**	**-0.08**	100	0.14				
300	**-0.08**	**100**	**-0.06**	**200**	**-0.08**	130	0.14				

*Thermistor failed on 24 August 2014

9/16/2014 - 9/15/2015

Browns Lake PF1		Watson Lake PF1		Watson Lake PF2		Watson Lake non-PF		KENAI 29 ENE AWS 702590 Met Station Data			
Sensor depth (cm)	MAGT (°C)	Sensor depth (cm)	MAGT (°C)	Sensor depth (cm)	MAGT (°C)	Sensor depth (cm)	MAGT (°C)	MAAT (°C)	TDD Sums	FDD Sums	MASD (cm)
50*	---	10*	---	10	1.53	25*	---				
100	**-0.04**	25*	---	50	0.14	50*	---	3.24	2009.8	829.1	2.7
200	**-0.06**	50*	---	**100**	**-0.07**	100*	---				
300	**-0.07**	100[#]*	---	200[#]	-0.07	130*	---				

*Thermistor or data logger failure

[#]Permafrost thaw during observation period

916 Table 2. Permafrost plateau extent mapped in each study region in 1950, 1984, 1996, and ca. 2010. Analyzed wetland area for each
917 study region is given along with the number of features, total plateau area, mean plateau area, and plateau extent for each image
918 observation year. In ca. 2010, images were acquired in 2011 (Mystery Creek and Watson Lake), 2012 (Tustumena Lake), and 2013
919 (Browns Lake).

920

Study Region	Wetland Area (ha)	1950				1984				1996				ca. 2010			
		Number of Features	Total Plateau Area (ha)	Mean Plateau Area (ha)	Plateau Extent (%)	Number of Features	Total Plateau Area (ha)	Mean Plateau Area (ha)	Plateau Extent (%)	Number of Features	Total Plateau Area (ha)	Mean Plateau Area (ha)	Plateau Extent (%)	Number of Features	Total Plateau Area (ha)	Mean Plateau Area (ha)	Plateau Extent (%)
Mystery Creek	1562.0	212	511.5	2.4	32.7	237	457.7	1.9	29.3	335	292.6	0.9	18.7	321	232.3	0.7	14.9
Watson Lake	904.2	44	86.6	2.0	9.6	55	54.0	1.0	6.0	68	35.4	0.5	3.9	67	29.8	0.4	3.3
Browns Lake	1013.0	102	111.9	1.1	11.0	117	67.2	0.6	6.6	107	51.2	0.5	5.1	89	38.6	0.4	3.8
Tustemena Lake	1333.4	92	210.2	2.2	15.8	150	168.6	1.1	12.6	183	143.5	0.8	10.8	206	69.9	0.3	5.2
All Sites	4812.7	450	920.2	2.0	19.1	559	747.5	1.3	15.5	693	522.6	0.8	10.9	683	370.6	0.5	7.7

921

922

923 Table 3. Change in the extent of permafrost plateaus for each of the study regions between 1950
924 and ca. 2010, 1950 and 1984, 1984 and 1996, and 1996 and ca. 2010. Change is reported in
925 aerial units per year, proportional area change, percent change per year, and by the type of
926 change. Change type refers to whether the plateau loss occurred along the periphery of a feature
927 (lateral), in the centre of a feature (internal), or whether complete loss of a feature occurred. In
928 ca. 2010, images were acquired in 2011 (Mystery Creek and Watson Lake), 2012 (Tustumena
929 Lake), and 2013 (Browns Lake).
930

| Study Area | 1950 to ca. 2010 | | | | | |
| | Area Change (ha yr^{-1}) | Proportional Area Change (ha yr^{-1} 100 ha^{-1}) | Percent Change (% yr^{-1}) | Change Type | | |
				Lateral (%)	Internal (%)	Complete (%)
Mystery Creek	-4.6	-0.3	-0.9	86.2	3.3	10.5
Watson Lake	-0.9	-0.1	-1.1	90.9	0.8	8.3
Browns Lake	-1.2	-0.1	-1.0	77.2	0.3	22.4
Tustumena Lake	-2.3	-0.2	-1.1	86.0	1.7	12.3
All Sites	-9.2	-0.2	-1.0	85.1	1.5	13.4

| Study Area | 1950 to 1984 | | | | | |
| | Area Change (ha yr^{-1}) | Proportional Area Change (ha yr^{-1} 100 ha^{-1}) | Percent Change (% yr^{-1}) | Change Type | | |
				Lateral (%)	Internal (%)	Complete (%)
Mystery Creek	-1.6	-0.1	-0.3	88.8	5.2	5.9
Watson Lake	-1.0	-0.1	-1.1	91.7	1.4	6.9
Browns Lake	-1.3	-0.1	-1.2	89.0	0.6	10.1
Tustumena Lake	-1.2	-0.1	-0.6	94.1	2.1	3.8
All Sites	-5.1	-0.1	-0.6	91.0	2.3	6.7

| Study Area | 1984 to 1996 | | | | | |
| | Area Change (ha yr^{-1}) | Proportional Area Change (ha yr^{-1} 100 ha^{-1}) | Percent Change (% yr^{-1}) | Change Type | | |
				Lateral (%)	Internal (%)	Complete (%)
Mystery Creek	-13.8	-0.9	-3.0	87.1	1.8	11.2
Watson Lake	-1.6	-0.2	-2.9	88.7	0.6	10.7
Browns Lake	-1.3	-0.1	-2.0	84.0	0.1	16.0
Tustumena Lake	-2.1	-0.2	-1.2	85.1	2.9	12.0
All Sites	-18.7	-0.4	-2.5	86.2	1.3	12.5

| Study Area | 1996 to ca. 2010 | | | | | |
| | Area Change (ha yr^{-1}) | Proportional Area Change (ha yr^{-1} 100 ha^{-1}) | Percent Change (% yr^{-1}) | Change Type | | |
				Lateral (%)	Internal (%)	Complete (%)
Mystery Creek	-4.0	-0.3	-1.4	82.7	3.0	14.3
Watson Lake	-0.4	-0.1	-1.1	92.2	0.5	7.3
Browns Lake	-0.7	-0.1	-1.4	58.7	0.1	41.2
Tustumena Lake	-4.6	-0.3	-3.2	78.7	0.2	21.1
All Sites	-9.5	-0.2	-1.8	78.1	1.0	21.0

931

40

932 Table 4. Mean annual, mean summer (May to September), and mean winter (October to April)
933 air temperature for the three remotely sensed image observation periods compiled from the
934 Kenai Municipal Airport (WBAN 26523) and estimated from the MRC station (Kenai 29 ENE -
935 AWS 702590).

936

Remote Sensing Time Period	Mean Annual Air Temperature (°C)		Mean Summer Air Temperature (°C)		Mean Winter Air Temperature (°C)	
	Kenai Airport	MRC	Kenai Airport	MRC	Kenai Airport	MRC
1950 to 1984	1.12	0.59	9.92	10.39	-5.29	-6.54
1984 to 1996	1.77	1.31	10.28	10.78	-4.37	-5.52
1996 to 2015	2.34	1.86	10.81	11.31	-3.77	-4.95

937
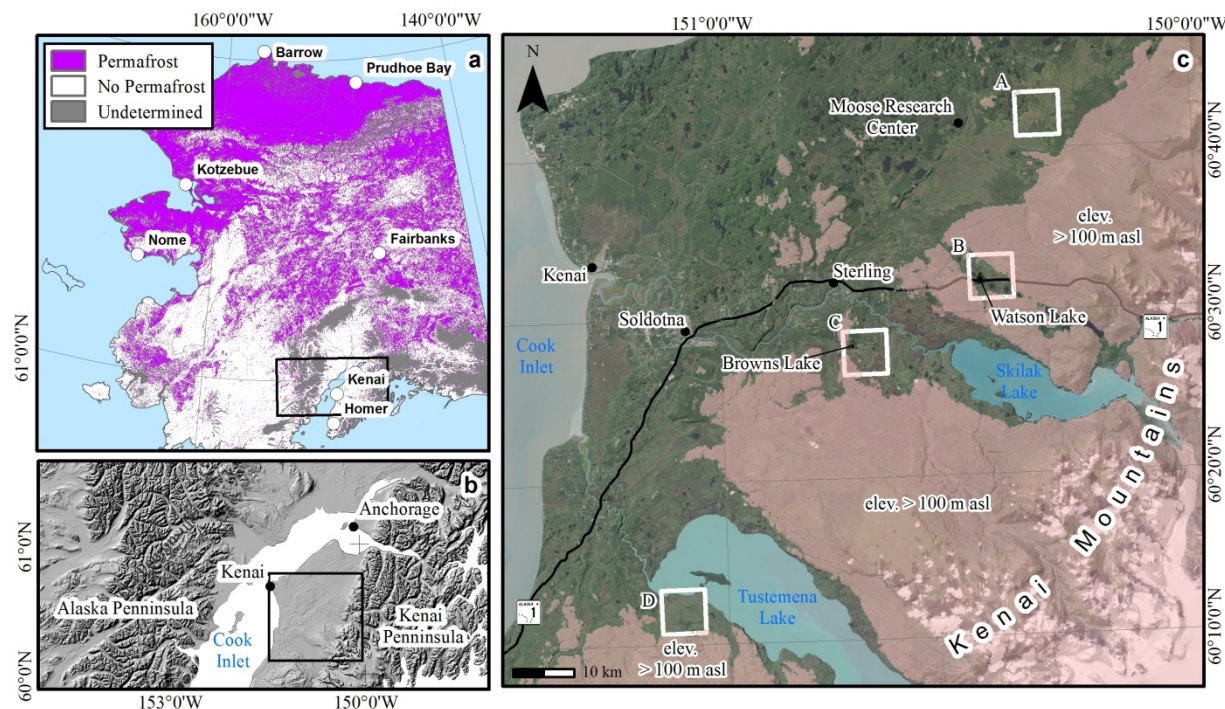
Figures

Figure 1: Study area figure. (a) Recent permafrost map of Alaska (Pastick et al., 2015) indicating permafrost presence (purple) and absence (white) in the upper one meter of the ground surface. (b) Hillshade relief image showing a portion of southcentral Alaska. The study region on the Kenai Peninsula lowlands is shown with the black box outline. (c) The portion of the Kenai Peninsula lowlands where field studies and remotely sensed observations were conducted. Ground temperature observations were collected at the Browns Lake and Watson Lake sites. The remote sensing change detection areas are shown with a white box: (A) Mystery Creek, (B) Watson Lake, (C) Browns Lake, and (D) Tustumena Lake wetland complexes.

948
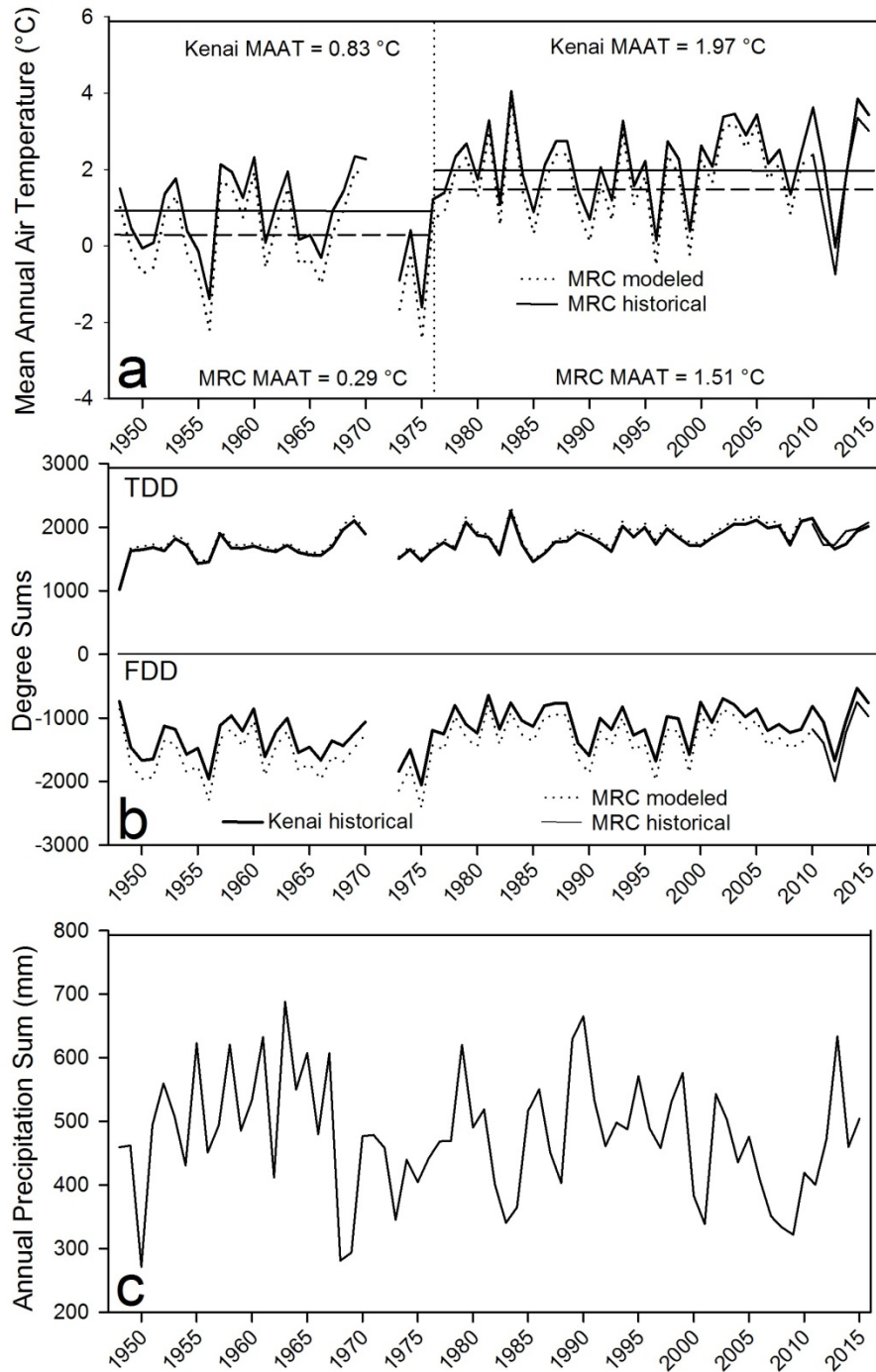
Figure 2:   a) Historical (1948-2015) mean annual air temperature compiled from Kenai
Municipal Airport (WBAN 26523) hourly surface data and interpolated (broken) and measured
(solid) mean annual air temperature for the MRC station (Kenai 29 ENE AWS 702590). b)
Thawing degree day (TDD) and freezing degree day (FDD) sums for 1948-2015 derived from
historical and interpolated daily mean temperature. c) Cumulative annual precipitation data from
the Kenai Municipal Airport (WBAN 26523) between 1948 and 2015.

955

956

Figure 3: Field photos of residual permafrost plateau landforms and thermokarst on the western Kenai Peninsula lowlands. (a) A forested permafrost plateau in the Browns Lake wetland complex. A thermokarst moat and drowning black spruce trees in the (b) Browns Lake and (c) Watson Lake wetland complexes.

961

962
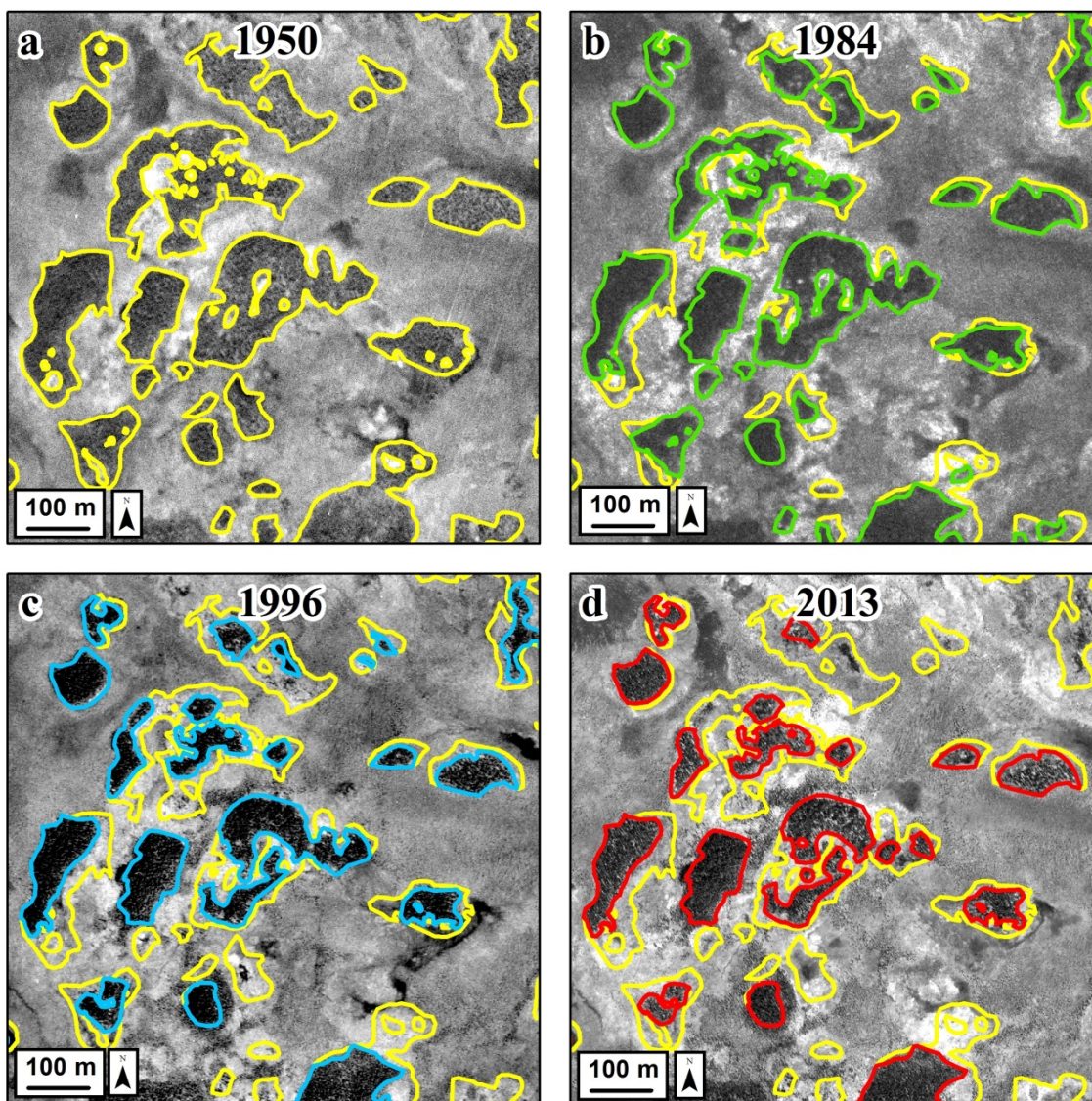
Figure 4: Time series documenting the extent of a subset of permafrost features in the Browns Lake wetland complex in (a) 1950, (b) 1984, (c) 1996, and (d) 2013. Permafrost plateau extent in 1950 is shown as a yellow polygon in each frame and other time slices outlined as green (1984), blue (1996), and red (2013).

968

969
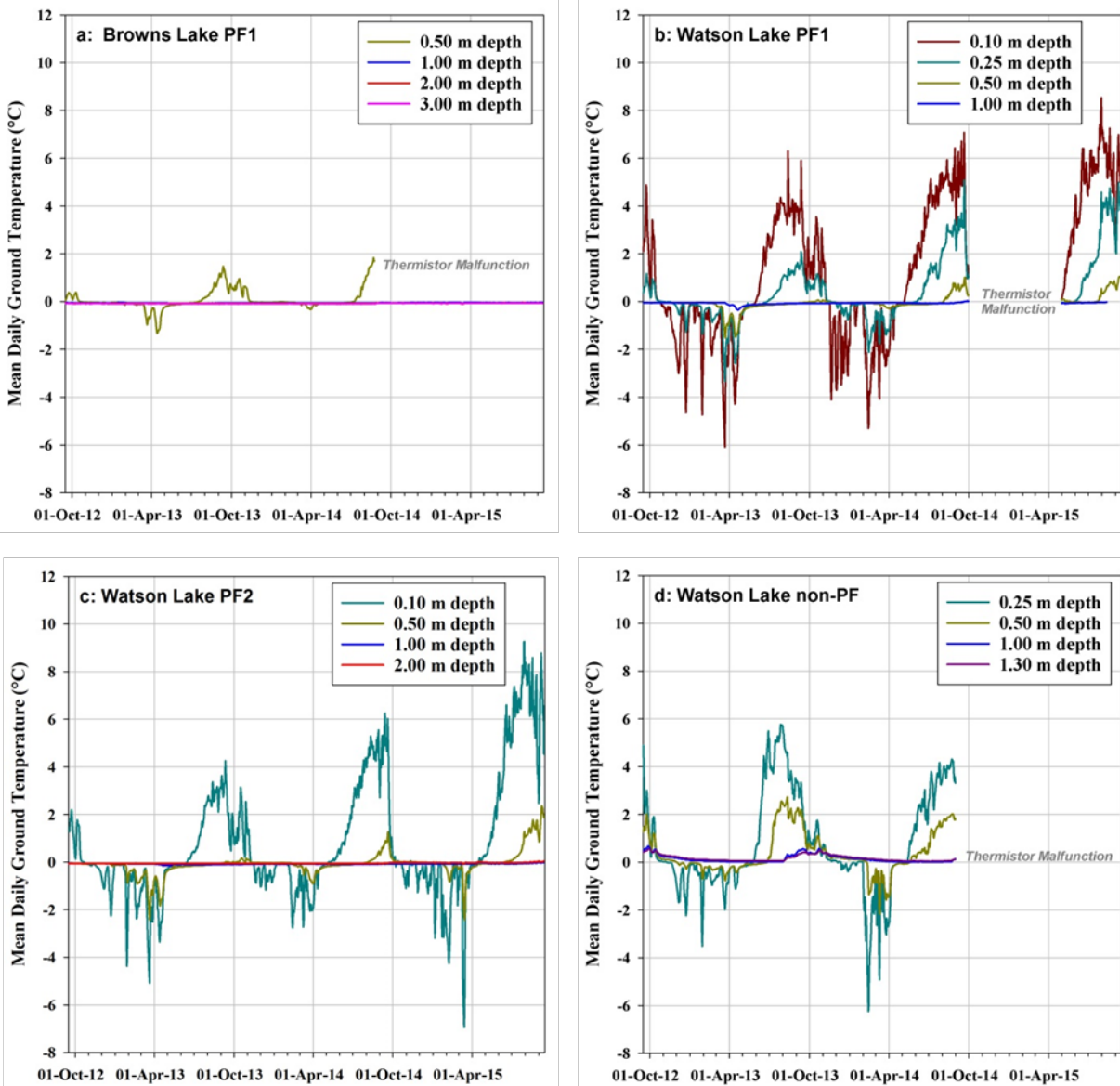
Figure 5: Mean daily ground temperature data plots for the four shallow boreholes on the western Kenai Peninsula lowlands for the period of 16 September 2012 to 15 September 2015: (a) Browns Lake PF1 site, (b) Watson Lake PF1 site, (c) Watson Lake PF2 site, and (d) Watson Lake non-PF site. All axes scales are the same but sensor depths vary among sites based on site characteristics. Missing data indicates sensor or thermistor failure.

975

976
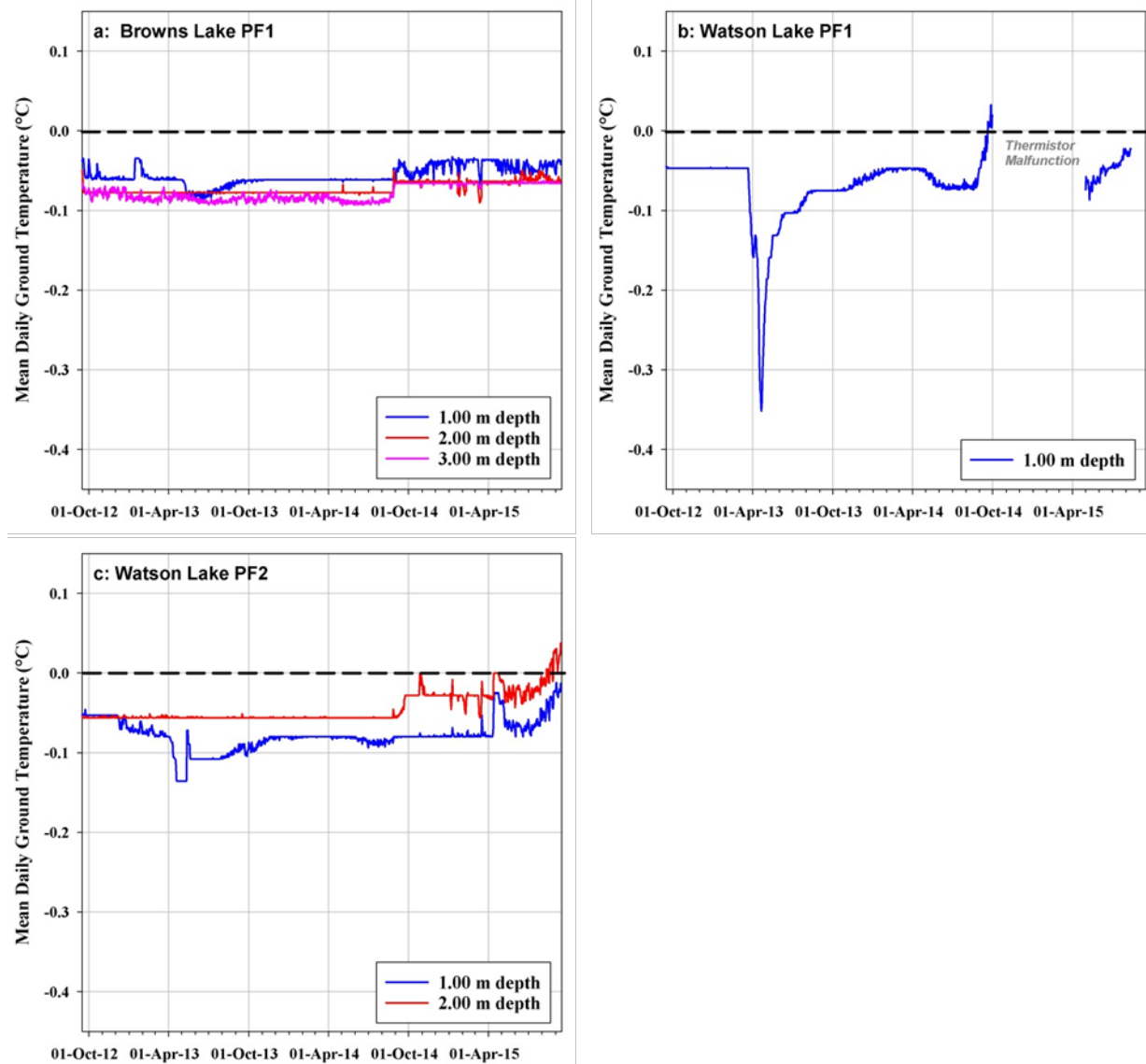
Figure 6: Mean daily ground temperature data plots indicating the presence of permafrost on the
western Kenai Peninsula lowlands for the period of 16 September 2012 to 15 September 2015:
(a) Browns Lake PF1 site, (b) Watson Lake PF1 site, and (c) Watson Lake PF2 site. Top-down
permafrost thaw occurred at Watson Lake PF1 during the fall of 2014 and bottom-up permafrost
thaw occurred at Watson Lake PF2 during the fall of 2015.

982

983
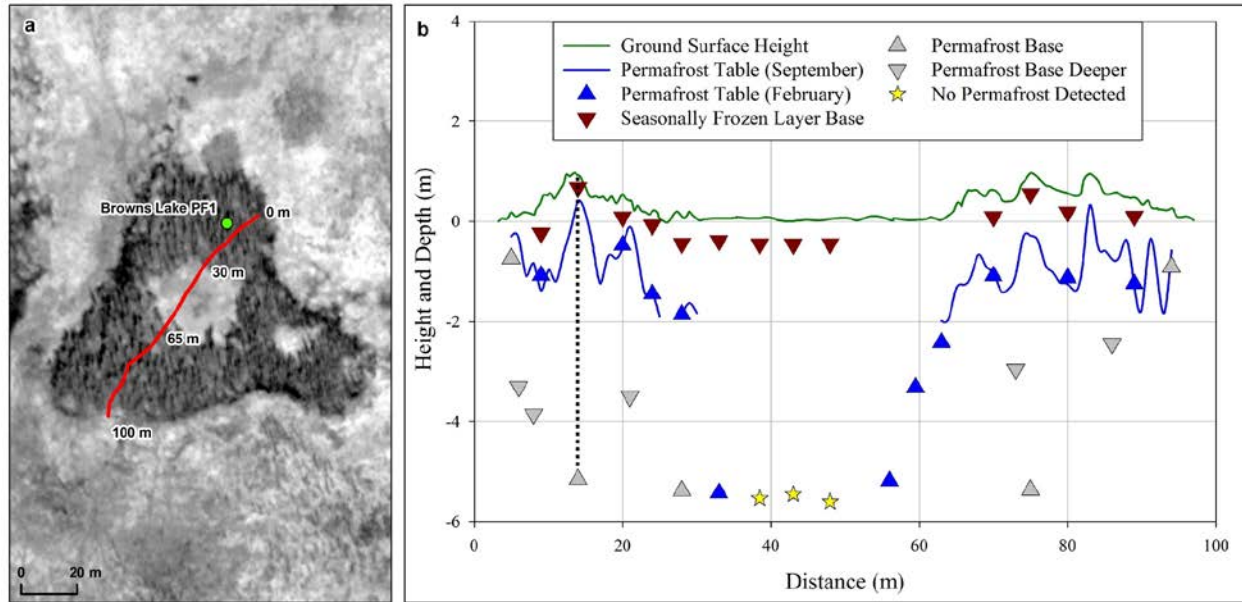
Figure 7: (a) High-resolution satellite image showing the permafrost plateau in the Browns Lake wetland complex where detailed field surveys were conducted as well as the location of the Browns Lake PF1 data logger (green dot). (b) A ~100 m transect across the Browns Lake PF1 permafrost plateau site showing ground surface height above the wetland (green line), depth to the permafrost table (blue line and blue arrows), permafrost thickness constraints (grey arrows), seasonally frozen ground depth (maroon arrows), and lack of permafrost (yellow stars) as measured by probing, drilling, and coring. Locations where the permafrost table exceeded 2.2 m from the ground surface (limiting depth for September surveys) are indicated with a non-existent blue line. Locations where the base of the permafrost was encountered are indicated with an upward looking grey triangle and those locations where it was not encountered, a downward looking grey triangle. The black dashed vertical line represents the location of the PF-BL-6 permafrost core.
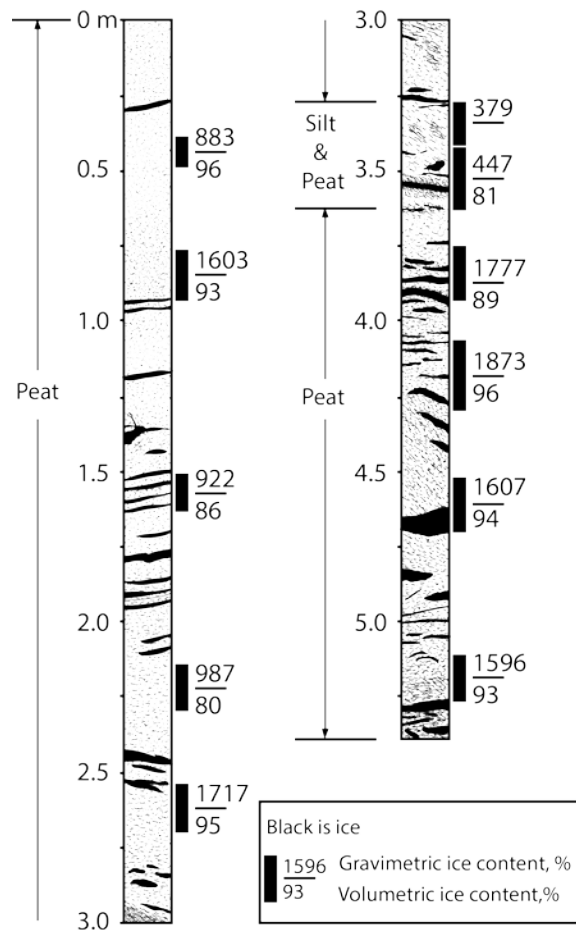
Figure 8: Cryostratigraphy and ice contents from borehole PF-BL-6 (inspired by Kanevskiy et al., 2014). The gravimetric and volumetric ice contents of the peat varied between 883–1873% and 80–96%, respectively, while they were 379–447% and 81%, respectively, in the silt and peat layer located between 3.32 m and 3.65 m.

1002
1003
1004 Figure 9: (a) Stratigraphic contact between the base of the frozen silt and peat layer occurring at
1005 3.65 m and the underlying frozen peat. (b) Example of organic-matrix microlenticular to
1006 suspended cryostructures developed in the peat below the stratigraphic contact shown in (a).
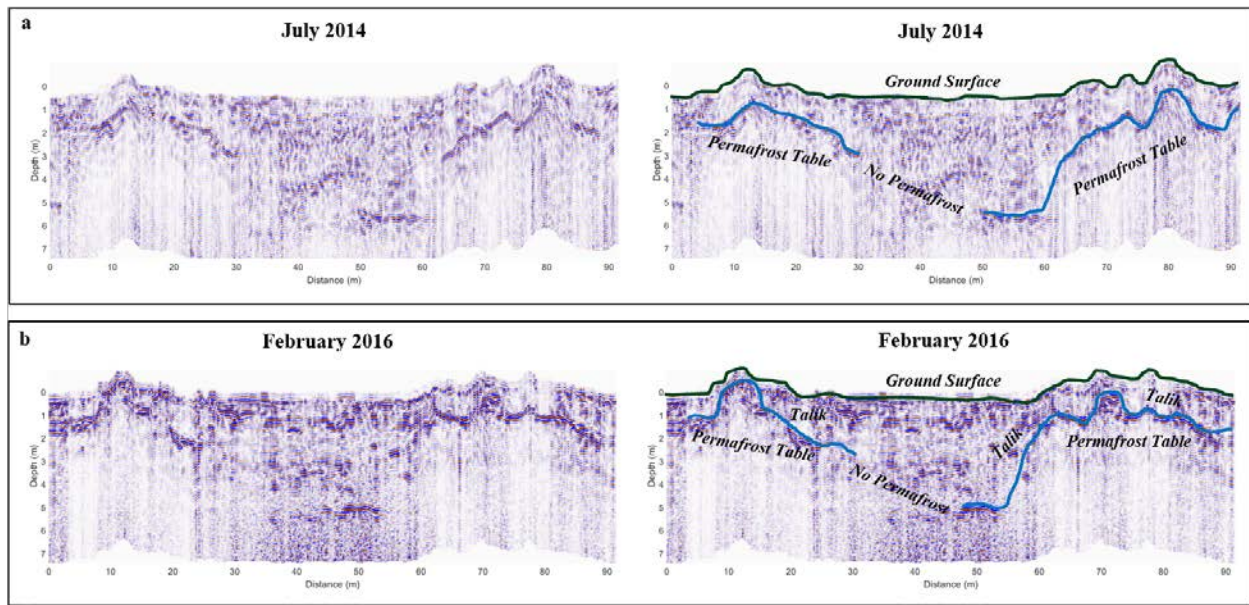
1009 Figure 10: GPR profiles at the intensive Browns Lake permafrost plateau (Fig. 7a) from a) late-
1010 July 2014 with Mala shielded 100-MHz antennas and b) mid-February 2016 with Sensors &
1011 Software unshielded bi-static 100-MHz antennas. Processed radargrams are on the left and
1012 processed, interpreted radargrams are on the right. Both summer and winter profiles clearly
1013 show reflectors associated with the permafrost table and in the case of (b) show the presence of a
1014 talik. However, we were unable to image the permafrost base using GPR. Note that the two
1015 GPR transects differ slightly in their orientation across the feature.
1016
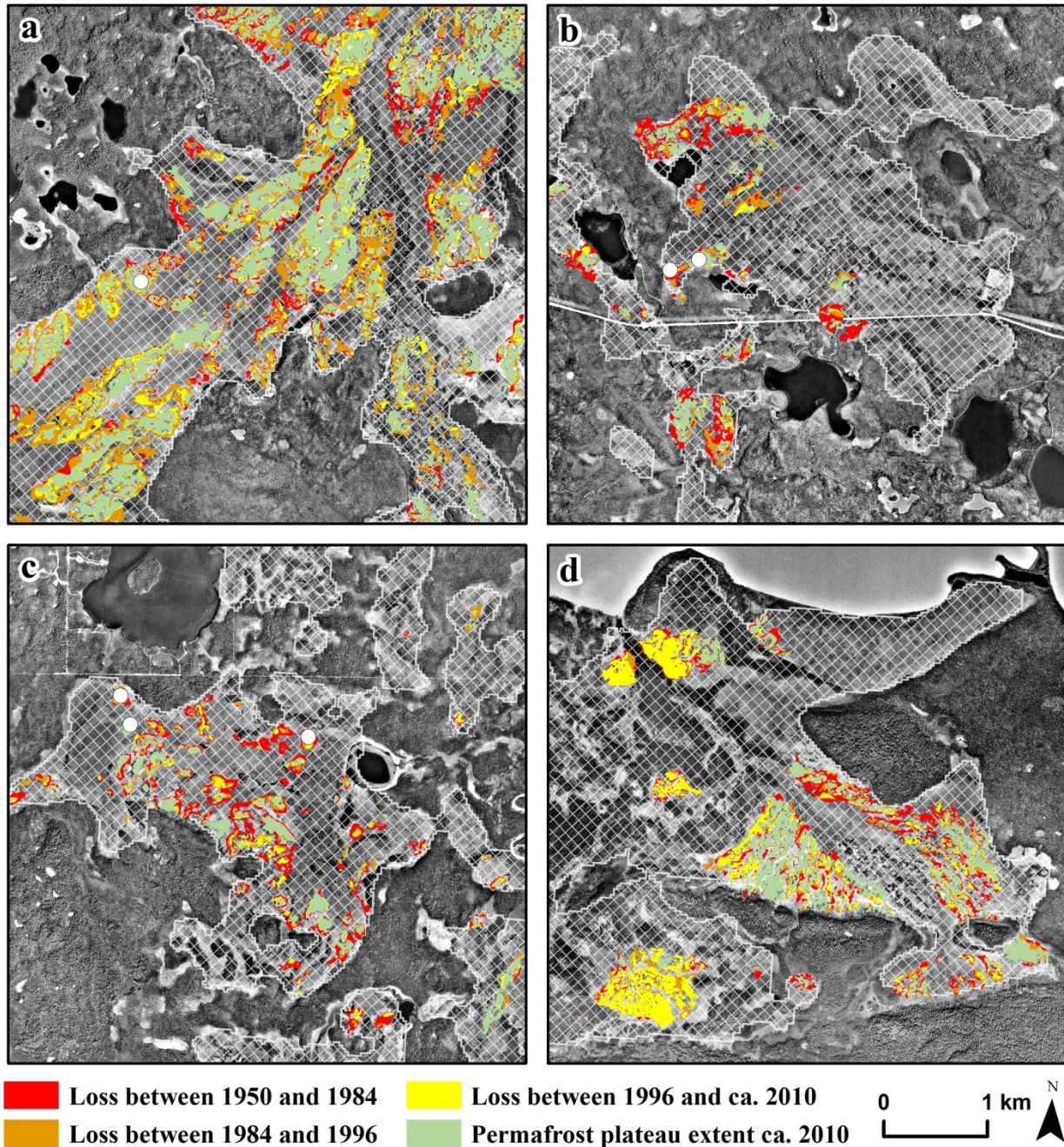
Figure 11: Spatial and temporal pattern of permafrost loss within four change detection areas: a) Mystery Creek, b) Watson Lake, c) Browns Lake, and d) Tustumena Lake. Red indicates feature loss between 1950 and 1980, orange is feature loss between 1984 and 1996, yellow is feature loss between 1996 and ca. 2010, and green is ca. 2010 permafrost plateau extent. The white dots indicate the location of field verified permafrost between 2009 and 2016. The hatched white polygons indicate the wetland extent where plateau features were mapped in each study area. Background imagery is the 1996 orthophotography.